SIEMENS

Report

**Power and Gas**
**Technology**
Siemens Nederland N.V. Hengelo



# SGT-600 Lube Oil System Simulation

## Matlab Simulink Model

*Name*: Stefan Klooster
*Student number*: s1196782
*Company*: Siemens Nederland N.V.
*Department*: Technology & Innovation
*Project Coordinator*: G. de Boer

Hengelo, The Netherlands
March 1st till May 31st 2016.

University of Twente
Mechanical Engineering
Engineering Fluid Dynamics
Prof.dr.ir. C.H. Venner

| | Date | Name | Dept. | Title |
|---|---|---|---|---|
| Prepared | 2016-05-31 | Stefan Klooster | PG DR TE PDT HGO | SGT-600 Lube Oil System Simulation |
| Checked | 2016-05-31 | Geert de Boer | PG DR TE PDT HGO | Matlab Simulink Model |
| Released | 2016-05-31 | Marcel Buse | PG DR TE PDT HGO | |

| | Size | Document no. | Revision | Page |
|---|---|---|---|---|
| **Siemens Nederland N.V.** | **A4** | **RD401101** | A | 1 of 46 |

 

# SGT-600 Lube Oil System Simulation

## Matlab Simulink Model

| | |
|---|---|
| Classification | RESTRICTED |
| Client | Internal |
| Project Title | SGT600 Lube Oil System |
| Project Number | ZIA-723 SPA08 SP04 WP17 |
| Product Type | SGT 600/700 |



 

***Stefan Klooster***

***s1196782***

Siemens Nederland N.V.
Energy Sector Oil & Gas
Industrieplein 3
7553 LL Hengelo
The Netherlands

Department: Technology & Innovation

Department Manager: M. Buse, marcel.buse@siemens.com
Phone +31 (0) 74 2402562
Mobile +31(0)6 12026270

Project Coordinator: G. de Boer, geert.de_boer@siemens.com
Phone +31 (0) 74 240 2397

March 1st till May 31st 2016.

University of Twente
Mechanical Engineering
Engineering Fluid Dynamics
Prof.dr.ir. C.H. Venner



 

# TABLE OF CONTENTS



 

## Executive Summary

The lube oil system in the SGT 600 has to supply oil of the correct pressure and temperature to the gas turbine bearings, the gear and the compressor bearings for lubrication and cooling. The lubrication oil used in the system is mineral based turbine oil ISO VG 46. The oil in the system goes through multiple components before the bearings and gear are reached. Two centrifugal pumps, which are driven by electric motors, pump the oil through a cooler, bypass line, 3 way temperature valve and a filter before the oil enters the bearings. All these components have a pressure loss (resistance) which depends on the flow that goes through the component. On the other side, the flow that is present in the system depends on the resistance of the total system.

To show this dynamic behaviour of the system, a simplified mathematical simulation model is required for the start-up of the lube oil system of the SGT 600. This model must calculate the flow and pressure in each part of the lube oil system. Furthermore, the bypass line over the cooler has an orifice plate which must take care of a pressure loss that is equal to the pressure drop of the cooler. The simulation model must provide a suitable selection tool for the orifice bore diameter of the bypass line.

The simulation tool used for this model is *Matlab Simulink*. To simulate the total lube oil system, the model is split into an iterative part and an integration part. For the total model, these two parts are coupled after both models are tested. The iterative part finds the flow in the total lube oil system and the integration part takes care of the coupling between the electric motors and the centrifugal pumps. This way, the start-up behaviour can be described.

From available datasheets it can be seen that the desired pressure upstream the bearings in the system does not correspond to the design flow and speed of the centrifugal pumps. So the centrifugal pumps do not operate at their best efficiency point. The simulation tool described in this report will predict the flow and the pressure at every component in the system.

The final model described in this report is capable of finding the pressure and flow at each component in the system. However, the final model contains a lot of assumptions which cannot be validated due to a lack of data. Also, the model is capable of showing the physical behaviour. This physical behaviour contains the distribution of the flow over parallel components, where the components with the lowest resistance gets the most flow. It also contains the dynamic behaviour where the resistance determines the flow in the system and the flow on its turn determines the resistance.

The final model is also capable of predicting the mentioned orifice diameter in the bypass line over the cooler. The model runs a script which calculates the desired diameter to get the same pressure loss over the bypass line as over the cooler.

 

## Nomenclature

| Symbol | Description | Unit |
|---|---|---|
| $\beta$ | Ratio of orifice hole diameter to pipe diameter | [-] |
| $\epsilon$ | Relative eccenctricity, $\epsilon = e/r$ | [-] |
| $\epsilon_r$ | Roughness | $[mm]$ |
| $\eta$ | Efficiency | [-] |
| $\mu$ | Dynamic viscosity | $[kg/ms]$ |
| $\omega$ | Angular velocity | $[1/s]$ |
| $\rho$ | Density | $[kg/m^3]$ |
| $A_{orif}$ | Cross sectional area orifice hole | $[m^2]$ |
| $C$ | Flow coefficient | [-] |
| $c$ | Radial clearance at neutral position | $[m]$ |
| $C_d$ | Discharge coefficient | [-] |
| $d$ | Diameter orifice hole | $[m]$ |
| $D$ | Pipe diameter | $[m]$ |
| $f_D$ | Darcy-Weisbach friction factor | [-] |
| $g$ | Gravitational acceleration | $[m/s^2]$ |
| $h$ | Head pressure | $[m]$ |
| $h_d$ | Design head pressure | $[m]$ |
| $h_{so}$ | Shut-off head pressure | $[m]$ |
| $h_{stat}$ | Static head pressure | $[m]$ |
| $J$ | Moment of inertia | $[kgm^2]$ |
| $l$ | Length of the half-bearing | $[m]$ |
| $L$ | Pipe length | $[m]$ |
| $N$ | Speed | $[RPM]$ |
| $p$ | Pressure | $[Pa]$ |
| $p_1$ | Pressure upstream orifice | $[Pa]$ |
| $p_2$ | Pressure downstream orifice | $[Pa]$ |
| $P_h$ | Hydraulic power | $[W]$ |
| $P_{motor}$ | Power of electric motor | $[W]$ |
| $P_s$ | Shaft power | $[W]$ |
| $Q$ | Volume flow | $[m^3/s]$ |
| $Q_d$ | Design flow | $[m^3/s]$ |
| $r$ | Ratio between max and design flow | [-] |
| $r$ | Journal radius | $[m]$ |
| $Re$ | Reynolds number | [-] |
| $s$ | Stable flow range | [-] |
| $t$ | Time | $[s]$ |
| $T$ | Torque | $[Nm]$ |
| $T_{motor}$ | Torque delivered by electric motor | $[Nm]$ |
| $T_{pump}$ | Torque required by pump | $[Nm]$ |
| $V$ | Velocity | $[m/s]$ |



 

# 1 Introduction

The Siemens SGT-600 is a heavy-duty industrial gas turbine designed and built to meet requirements for low life-cycle cost. The lube oil system in the SGT 600 has to supply oil of the correct pressure and temperature to the gas turbine bearings, the gear and the compressor bearings for lubrication and cooling.

A simulation model is required for the start-up of the lube oil system of the SGT 600. This model must calculate the flow and pressure in each part of the lube oil system during start-up. The simulation tool used for this model is *Matlab Simulink*. To simulate the total lube oil system, the model is split into two parts and these are coupled after both models are tested.

The first model is an iterative model, which finds the flow in a system with centrifugal pumps and an orifice plate, which sets the resistance in the system. This iterative model is described in section 4.2. The second model is an integration model, which is describe in section 4.3. This model couples the electric motor to the centrifugal pumps. Due to the torque delivered by the electric motors, the pumps accelerate. They will accelerate until the delivered torque is equal to the required torque by the pumps.

The two models described above are coupled to each other, which is described in section 4.4. Due to this coupling, the start-up of the lube oil system can be simulated. After this coupling is made, the system is extended towards the final model.

The final model contains the components which are present in the real system. These components all have a pressure loss (resistance) which depends on the flow that goes through the component. At the same time, the flow that goes through the system depends on the resistance of the system. The final model has the goal to find the flow and pressure everywhere in the system. The final model is described in chapter 5.

The flow and pressure every in the system are calculated and presented in chapter 6. Based on these results, conclusions and recommendations are described in chapters 7 and 8.

## 2 System description

The lube oil system in the SGT 600 has to supply oil of the correct pressure and temperature to the gas turbine bearings, the gear and the compressor bearings for lubrication and cooling. The lubrication oil used in the system is mineral based turbine oil ISO VG 46. In Figure 1, a simplified Piping and Instrumentation Diagram (P&ID) is shown. It can be seen that the lube oil system starts at the lube oil tank. In this tank, three centrifugal pumps are installed. These pumps are driven by three electric motors. In normal operation, two pumps work at 50%, and the third is in standby mode. After the pumps, a part of the oil goes through a cooler and the other part of the flow goes through a bypass line. This bypass line has an orifice plate, which is responsible for a pressure loss which must be the same as the pressure loss over the cooler. The flow through the cooler and the bypass are combined in the three way temperature valve. The function of this valve is to ensure a set temperature and regulate the flows over the bypass line and the cooler. This valve uses the temperature of the incoming flows to regulate the flow over the cooler and the bypass. After the three way temperature valve, the oil goes through a duplex filter. After the filter, the flow is split; a part goes to the gas turbine bearings, the gear and the compressor bearings. The other part of the flow goes into high pressure (positive displacement) pumps. The high pressure pumps deliver oil to the high pressure bearing of the gas turbine. After the oil lubricated the bearings and the gear, the oil flows back into the oil tank through drains.

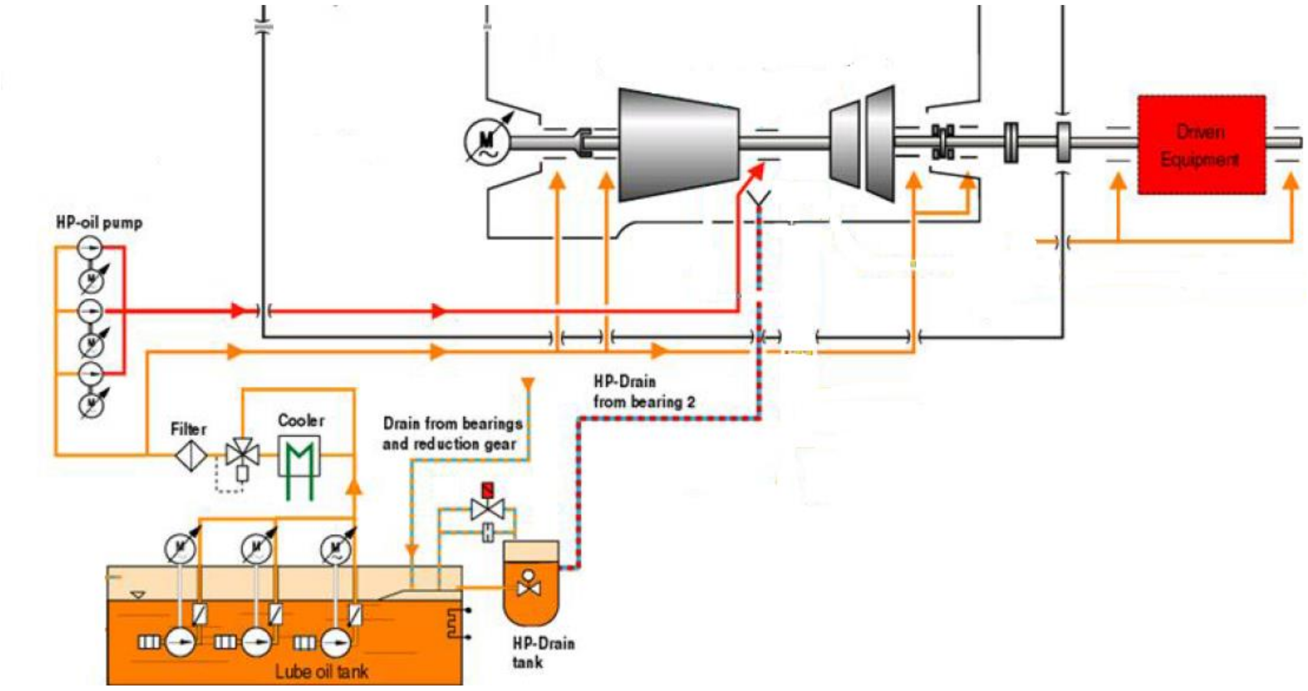


*Figure 1: Simplified P&ID of the lube oil system*

 

# 3 Assignment description

A simplified mathematical model of the system is required representing the physical behaviour of the lube oil system. Suitable assumptions have to be included representing the several components in the system and in particular the oil characteristics. To simulate the dynamic response of the system, the equations need to be solved using *Matlab Simulink*.

One characteristic of the lube oil system is formed by a bypass line around the cooler which regulates the oil flow. This bypass line contains a flow restricting orifice. The sizing of this orifice depends on the system characteristics. Having a suitable simulating tool for the system enables a suitable selection of the orifice bore size.



 

# 4 Simulation model

To simulate the lube oil system, first some assumptions have to be made in order to get a clear vision of what has to be simulated. This is done in section 4.1. After these assumptions, in section 4.2, an iterative model is explained in which the operating point of an centrifugal pump is found at a constant speed. Then an integration model is described in section 4.3. This model is used to simulate the start-up of the pumps, which are driven by electric motors. These models are then coupled and extended in section 4.4 in order to simulate the complete lube oil system.

## 4.1 General assumptions

The simulation model has to find the flow in the system together with the resistance in the system. Assumptions made for this model are:

- The resistance in the system will also be affected by temperature changes in the system, because the viscosity is dependent on the temperature. However, for all the models in this report, a constant temperature is assumed during start-up of the lube oil system. This is done because the total time for start-up is relatively short and only a small amount of the total oil will be heated during the start-up, so the bulk temperature in the oil tank will hardly change.
- It is also assumed that oil is present everywhere in the system when the system is started. This has the consequence that a pressure difference in the system directly leads to a flow. So the model is not sequential, where the flow would start in the pumps and move through the system.
- The high pressure part of the lube oil system is not taken into account for the simulation model. This is done because this is a separate loop, which has not much effect on the rest of the system. The high pressure bearing is simulated as a normal gas turbine bearing.

The lube oil system that is eventually going to be simulated in this report is shown in Figure 2, so without the high pressure part.

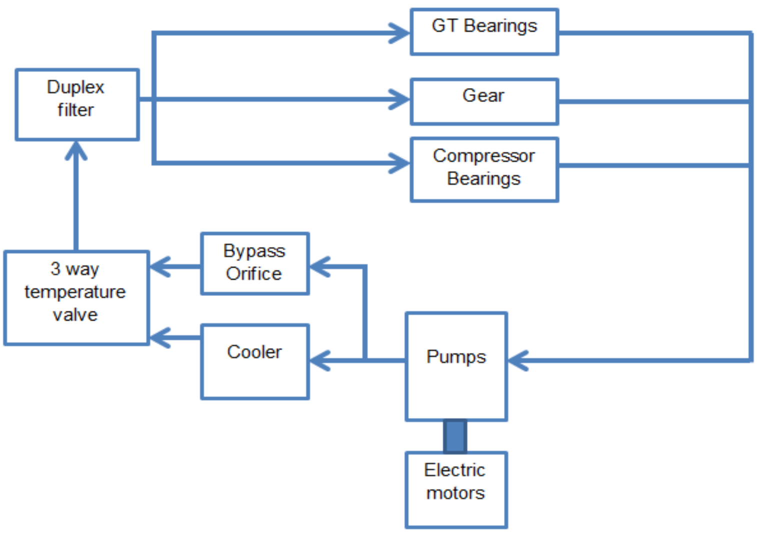


*Figure 2: Model to be simulated*

## 4.2 Iterative model

The first model is made to find the flow in a system with a pump at constant speed and an orifice plate. A centrifugal pump is a rotating machine in which flow and pressure are generated dynamically. An orifice plate is a device which is used to measure the flow rate, to reduce the pressure or to restrict the flow. In this case, the orifice plate is used to restrict the flow. The basic model is shown in Figure 3. The inlet pressure for the pump is equal to atmospheric pressure, because there is an oil tank in front of the pump, which has atmospheric pressure. The downstream pressure of the orifice plate is also equal to the atmospheric pressure. This is integrated in the blocks of the centrifugal pump and the orifice plate. It can be seen that the orifice plate states the flow in the system based on a pressure difference and the pressure delivered by the pumps on its turn depends on the flow in the system. With this iterative model, the intention is to find the operational point of the centrifugal pumps at a constant speed, so both the flow and the pressure in the system.

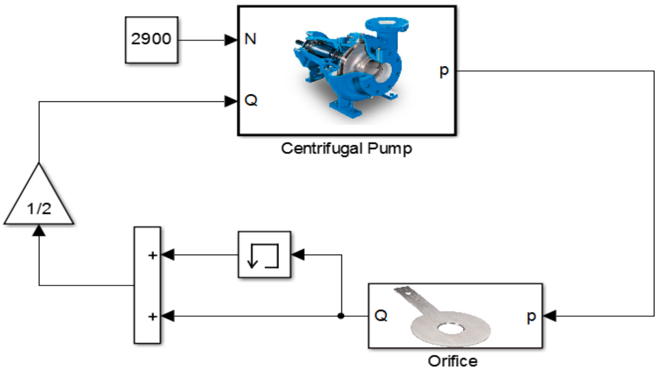


*Figure 3: Iterative model*

### 4.2.1 Centrifugal pump

The system makes use of two centrifugal pumps, which operate in parallel. From the datasheet of the pump, shown in Attachment 1, the data of the pumps in this model are approximated. For the designed speed ($2900\ RPM$) the flow-head curve for two parallel pumps is given. The design flow for the centrifugal pump is $Q_d = 96\frac{m^3}{h}$, where the design head pressure is equal to $h_{op} = 61.3\ m$. The design flow is a design parameter for the centrifugal pumps. This does not mean that the flow in the system is equal to this flow. The flow depends on the resistance in the system. If there is a lot of resistance in the system, the flow will be small and vice versa.

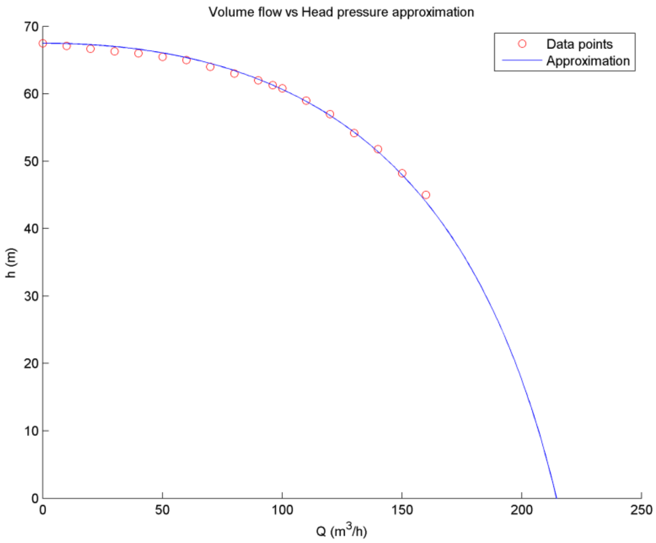


*Figure 4: Approximation flow-head curve of the pumps*

 

For the approximation of the flow-head curve of the pump, a method is used which uses the design- and maximum flow and head of the pump. Based on these parameters, the curve for the centrifugal pump is made. In Attachment 2 this method is explained in more detail and the result of the approximation is shown in Figure 4. It can be seen that the approximation intersects all the data points, which were read from the curve in Attachment 2. For the last part of the curve, approximately above $Q = 165\frac{m^3}{h}$, no more data points are known. For this part of the curve, the head delivered by the pump drops to zero, which means that the pump does not increase the pressure anymore. It is undesirable for the pumps to operate in this part of the curve.

From the head pressure delivered by the pump, the pressure in the system can be calculated with [1]:

$$p = \rho g h$$

This pressure goes towards the orifice plate, where a pressure-flow relation is used to calculate the flow in the system.

### 4.2.2 Orifice plate

An orifice plate can regulate the flow in a system. Volume flow rates through an orifice plate can be calculated with the *orifice equation* [2]*:*

$$Q = CA_{orif}\sqrt{\frac{2(p_1 - p_2)}{\rho}}$$

In this equation, $C$ is the flow coefficient. In Attachment 3, this coefficient is described in more detail. The flow is thus calculated with the pressure drop over the orifice. The upstream pressure ($p_1$) is found from the pumps and the downstream pressure ($p_2$) is atmospheric pressure, since that is equal to the pressure in the oil tank.

### 4.2.3 Iterative scheme

To find the operational point of the centrifugal pump, an iterative scheme is used. This is needed because the flow and pressure in the pump are generated dynamically. This is done by giving an initial guess for the flow and correcting the flow with the new computed flow. This is done by adding two successive iterations steps and taking the average of this, which can also be seen in Figure 3. The initial guess is chosen in the memory block in the system. Based on this initial guess, a pressure is calculated in the pumps. When an initial guess for the flow is taken low, the pump will deliver a high head. This will result in a large pressure drop over the orifice plate and thus a large flow. By adding this new flow to the initial guess and averaging it, the flow stays within the boundaries of the pump. At the new calculated large flow, the pump will deliver a low head and this will result in a small flow. Then the circle starts again, where a small flow will result in a high head pressure and thus a large flow. The same will work vice versa, when a too high initial guess is taken too high.

In the method described above, the operational point of the pump is found by moving over the pump curve. This is shown in Figure 5, where $Q_n$ is the initial guess of the flow. $\tilde{Q}_{n+1}$ is the new computed flow as a consequence of the initial guess and $Q_{n+1}$ is the average of these two and this is used as a new initial guess. This method is repeated until the difference between two successive iteration steps is smaller than a given percentage. The converging behaviour of this method is shown in Figure 6.

The number of iterations needed to converge is strongly dependent on the initial guess. As you would expect, the better the initial guess, the less iterations are needed for the same difference in two successive iteration steps.

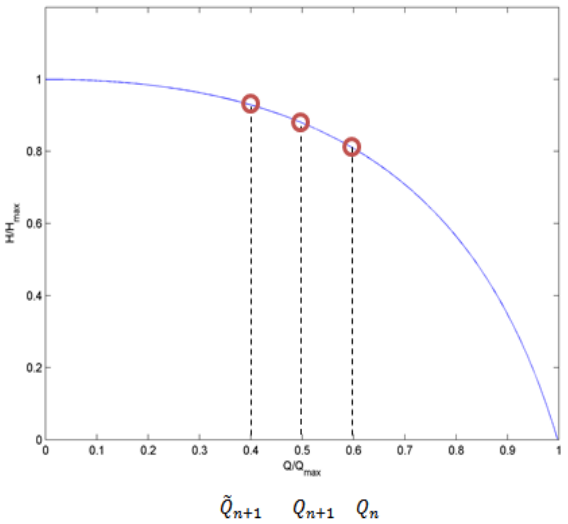


*Figure 5: Finding the operational point of the pumps*

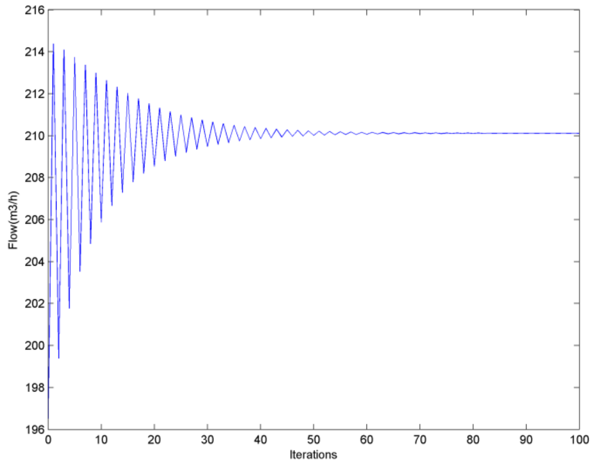


*Figure 6: Converging flow in the system*

## 4.3 Integration model

To couple the pump and the electric motor, a model is made as shown in Figure 7. The coupling between the two blocks is made with the torque. This coupling takes care of the acceleration of the pump due to the torque that the electric motor delivers. For this model, the input flow for the pumps is a ramp, which starts at zero flow and stops at the design flow; $Q_d = 96\ m^3/h$.

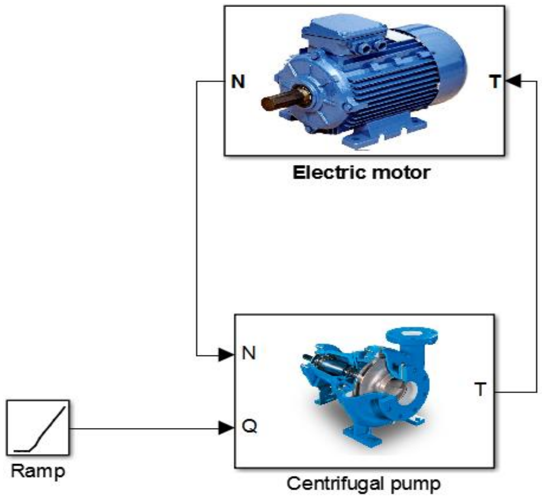


*Figure 7: Integration model*

 

### 4.3.1 Electric motor

The electric motors used in this model speeds up the centrifugal pumps. How fast the pumps accelerates depends on the requested torque of the pumps and the torque that the electric motors can deliver. The electric motors have a speed-torque relation which is shown in Figure 8. This figure is an approximation of the speed-torque curve in the datasheet, which is given in Attachment 4. In this attachment it can also be seen that the nominal torque of the electric motor is equal to $T_{nom} = 59\ Nm$ and the speed is equal to $N = 2971\ RPM$.
Because two centrifugal pumps, both powered by an electric motor, are present in the total system, the total delivered torque by the electric motor is multiplied by two in the system.

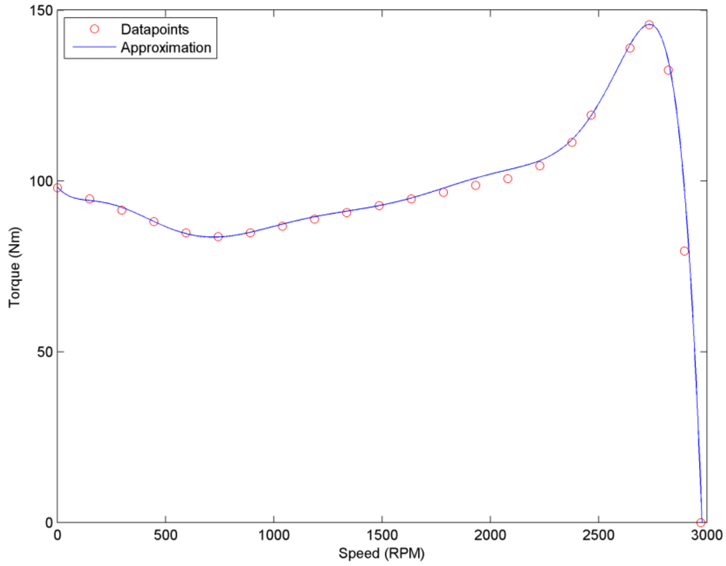


*Figure 8: Speed-Torque curve of the electric motor*

From this curve, the delivered torque at any moment is read at the actual speed. The delivered torque minus the requested torque of the pumps is divided by the moment of inertia of the pumps and the electric motors together. This leads to an angular acceleration for the pumps [3]:

$$\frac{T_{motor} - T_{pump}}{J} = \frac{\mathrm{d}\omega}{\mathrm{d}t}$$

This acceleration is integrated to get the angular velocity of the pumps. The angular velocity can be rewritten to a speed (RPM). When the pump is at a new speed, the pumps do also require more torque. The required torque of the pumps will be explained in section 4.3.2. With the new required torque of the pumps, again an angular velocity is calculated as described above. This leads to acceleration of the pumps until the delivered torque and the required torque are equal. Then a steady state is reached, where the pumps function at a constant speed.
The Simulink model of the electric motor as described above is given in Figure 9. Here, the block *T_n_motor* contains the speed-torque torque. The speed is the input and the delivered torque is read from the curve.

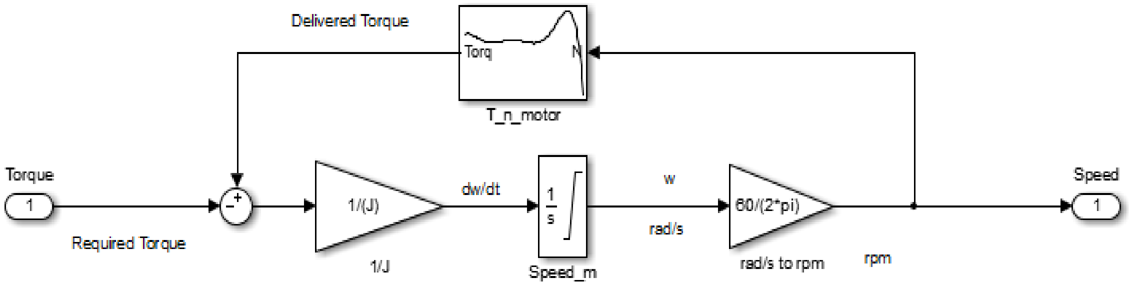


*Figure 9: Simulink model of the electric motor*

From the delivered torque and the speed of the electric motor, the power that is delivered by the electric motor can also be calculated [3]:

$$P_{motor} = \frac{2\pi}{60} NT$$

### 4.3.2 Centrifugal pump

The centrifugal pump is already described in section 4.2.1. However, this is only for a constant speed. Because the total model is about the start-up of the lube oil system, the flow-head curve of the pumps is scaled with the speed. This is done with the so-called affinity laws. The affinity laws are valid for a constant efficiency, which is assumed for this situation.
The affinity laws state that the flow is proportional to the speed [1]:

$$\frac{Q_1}{Q_2} = \frac{N_1}{N_2}$$

The head pressure is proportional to the square of the speed:

$$\frac{h_1}{h_2} = \left(\frac{N_1}{N_2}\right)^2$$

The flow-head curve for the pumps for different speeds is given in Figure 10. Here, the designed speed is given with the red curve and the other curves are different speeds. The speeds are plotted from $N = 0\ RPM$ to $N = 2900\ RPM$ with a difference of $100\ RPM$ between them.

 

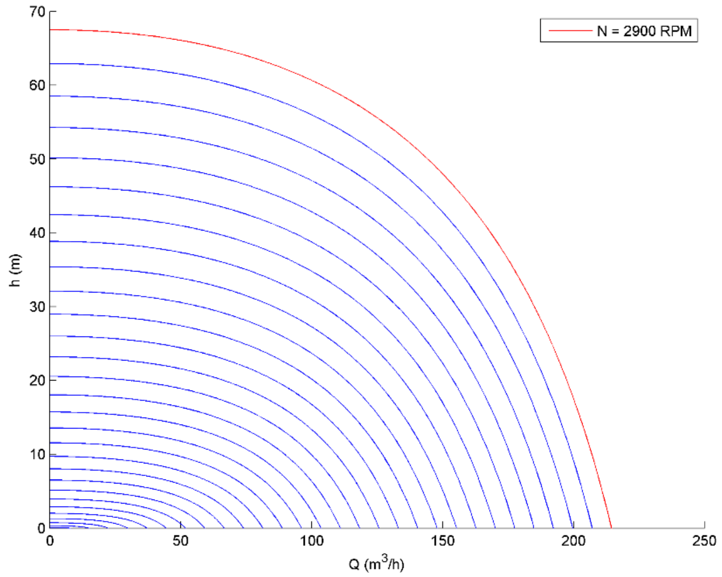


*Figure 10: Flow-head curve of centrifugal pumps for different speeds*

***Torque***

For the acceleration of the pumps, the required torque of the pumps has to be calculated. This torque depends on the shaft power $(P_s)$ and the speed $(N)$of the pump [4]:

$$T_{pump} = \frac{60}{2\pi}\frac{P_s}{N}$$

The scaling factor is the conversion for rounds per minute to angular velocity. The shaft power is found by the hydraulic power ($P_h$) divided by the efficiency ($\eta$) of the pump.

$$P_s = \frac{P_h}{\eta}$$

Here, the hydraulic power on its turn can be found with the following formula [4]:

$$P_h = \frac{Q\rho g h}{10^3}$$

Substituting these equations into the equation for the torque, it becomes:

$$T_{pump} = \frac{60}{2\pi}\frac{Q\rho g h}{\eta N}$$

***Check with data***

From the datasheet of the centrifugal pump (see Attachment 1) the torque and power of one centrifugal pump is known at a rotational speed of $n = 2900\ RPM$ and a flow of $Q = 48\ m^3/h$. In Table 1 this data is compared to the data from the model at the same speed and flow. It can be seen that the output of the model corresponds quite good to the datasheet. So the used formulas give the desired output.

| | Head [m] | Torque [Nm] | Shaft power [kW] |
|---|---|---|---|
| **Datasheet** | 61.3 | 40.1 | 12.17 |
| **Model** | 61.3 | 40.0 | 12.15 |

*Table 1: Comparison with data*

### 4.3.3 Result Integration model

Now that the torque of both the electric motors and the centrifugal pumps can be related, the centrifugal pumps can be accelerated by the electric motors. In Figure 11, the torque delivered by the motors and the torque required by the pumps are plotted. In Figure 12, the speed is plotted against the time. If these two figures are compared, it can be seen that when the torques intersect, the speed becomes constant, which was to be expected. The difference between the required and delivered torque is the stop criteria for this model. If the difference between these torques is smaller than a certain given percentage (0.01 % here), the model stops because steady state is reached.

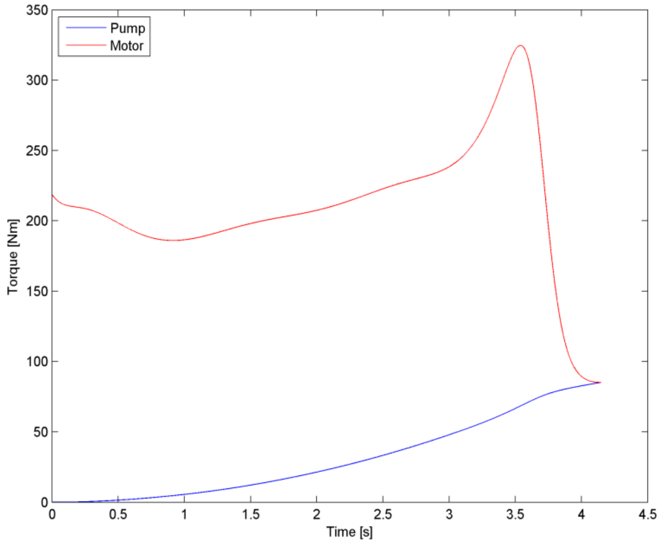


*Figure 11: Torques of the pumps and electric*

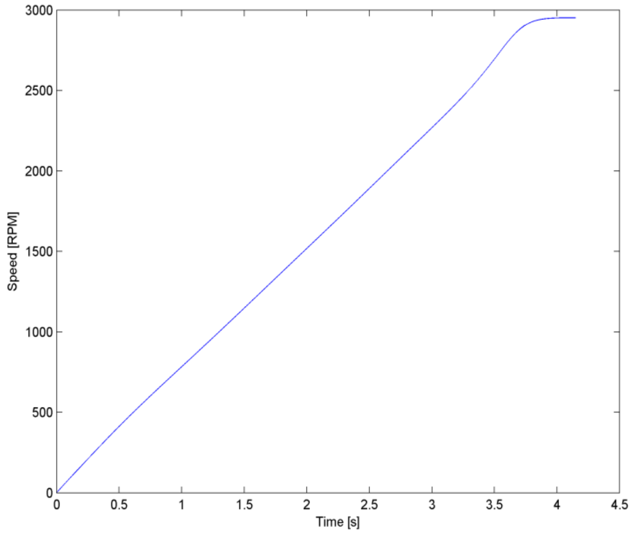


*Figure 12: Speed of the pumps*

***Power check***

With the equations for the power described above, the power that is required by the pumps and the power that is delivered by the electric motors are calculated. These powers are shown in Figure 13. When the system reaches steady state, the required and delivered power are the same. This shows that no energy is lost in the system.

 

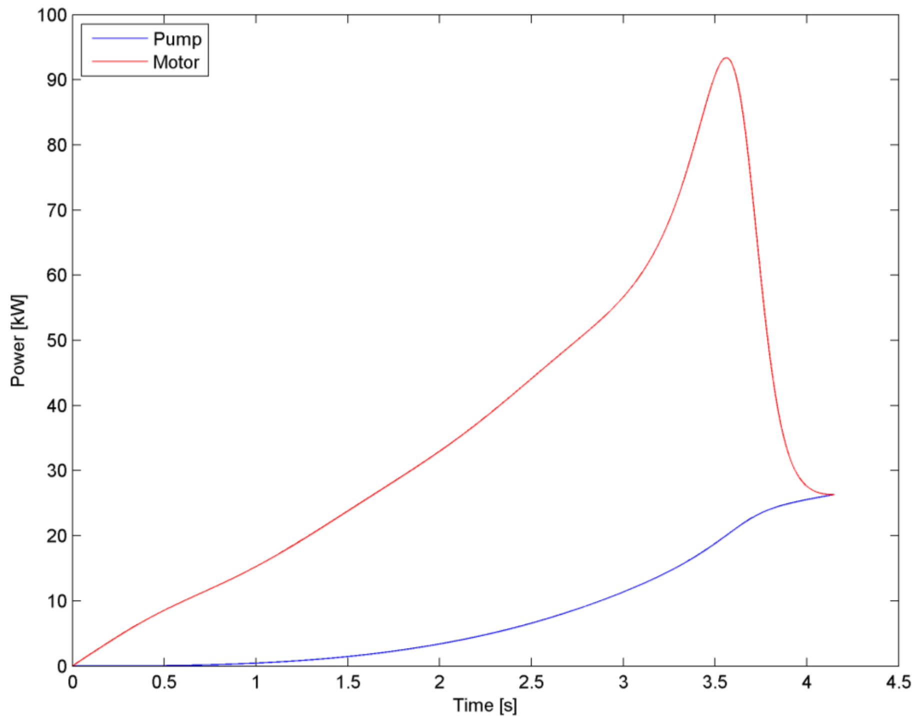


*Figure 13: Power of the pumps and the electric motors*

## 4.4 Total model

Now that the iterative model and the integration model are tested, they can be coupled. This is done in *Matlab Simulink* with a *While-iterator block.* This block gives a separation between the integration model and the iterative model. At a certain time step, the iterative model is running until the difference between two successive iteration steps is smaller than $0.01\%$. When this difference is met, the integration model goes to the next time step. This way, the total flow in the system is found for every time step. The total model now gives a start-up of the centrifugal pump, where the flow and pressure are found at every time step.

### 4.4.1 Model extension

Now, the basis for the total lube oil system is described and the model can be extended in order to simulate the real lube oil system, which was described in chapter 2. A first step is to simulate parallel flows in the system, where the resistance of the parallel lines takes care of the division of the total flow. After that, flow feedback is introduced in the system. This is necessary because the pressure loss of the components in the system in front of the bearings and gear are flow dependent, which will be explained in chapter 5.

 

### 4.4.2 Parallel flow

For the parallel flow, multiple resistances are used to simulate the behaviour. It is assumed that the pressure at the end of a junction is the same as at the inlet of the junction, so there is no pressure loss when a flow is divided. The pressure that goes into both parallel lines is thus the same and the resistance in the line determines the flow in that line. The line with the highest resistance gets the least flow and vice versa. The flows over both lines are added and the total flow enters the centrifugal pump. This principle can be used in the total system, where there are parallel flows after the filter.

### 4.4.3 Flow feedback

As will be shown in chapter 5, the pressure loss over the cooler, 3 way valve and filter are flow dependent. This makes it is necessary to have feedback of the total flow into these systems. This feedback is made on basis of mass conservation for incompressible fluids. The conservation of mass in a fluid is given by [5]:

$$\frac{\partial}{\partial t}\rho + \nabla \cdot (\rho u) = 0$$

For an incompressible fluids, this reduces to:

$$\nabla \cdot u = 0$$

It can be seen that this equation does not have a time dependency. Therefore, in this model, the conservation of mass is taken care of by feeding the total flow, calculated at the end of the system, directly back to the components in the beginning of the system. So at each time step, the conservation of mass is satisfied, because at each time step the total flow over the components in the system is equal to the total flow that enters the centrifugal pumps. This way, the pressure loss over these components can be calculated as a function of the flow.

### 4.4.4 Conditions

For the results, it is important to know which data is known. From Attachment 5 it is known that the pressure after the filter is equal to $p = 1.8\ barg$. Furthermore it is known from internal documents that the ratio of flows over the gas turbine bearings, gear and compressor bearings is 1:1:2/3. The gas turbine bearings and the gear thus get the same amount of flow and the compressor bearings get 2/3 of that flow. This means that the resistance over the gas turbine bearings and over the gear are equal and the resistance over the compressor bearings is larger.

From internal documents the maximum pressure losses over the cooler, 3 way temperature valve and the filter are known for the design flow. For the simulation these values are used, which gives the worst-case scenario of pressure loss in the system. In Table 2 the maximum pressure losses for the mentioned components are shown.

| Component | Maximum pressure loss for design flow |
|---|---|
| Cooler | $\Delta p_{max} = 0.869\ bar$ |
| 3 way temperature valve | $\Delta p_{max} = 0.1\ bar$ |
| Filter | $\Delta p_{max} = 0.36\ bar$ |
| **Total** | $\boldsymbol{\Delta p_{max} = 1.329\ bar}$ |

*Table 2: Maximum pressure loss for several components*

From this data, together with the data of the centrifugal pumps, it can already be seen that the system will not operate at the design flow. Because at the design flow and speed of the centrifugal pumps, a head pressure of $h = 61.3m$ will be delivered, which corresponds to a pressure of $p \approx 5.3\ barg$. At the design flow, the pressure loss over the components is found to be $\Delta p = 1.329\ bar$, as was shown in Table 2. The pressure after the filter will then approximately be $p = 3.9\ barg$. This does not correspond to the previously mentioned $p = 1.8\ barg$ behind the filter.

For this report, it is chosen to use the pressure behind the filter and the pressure losses of the components as leading design parameters. This has the consequence that the flow in the system will be greater than the design flow, because a greater flow will result in a lower pressure delivered by the pumps. Furthermore, the ratios between the parallel flows are used as design parameters.
The goal of the final model is to find the flow in the system at which the condition for the pressure behind the filter is met. This will result in a pressure delivered by the centrifugal pumps . This gives a dynamic system where the resistance in the system determines the flow in the system and the flow in the system on its turn determines the resistance in the system, because the pressure losses in the components are flow dependent.



 

## 5 Final model

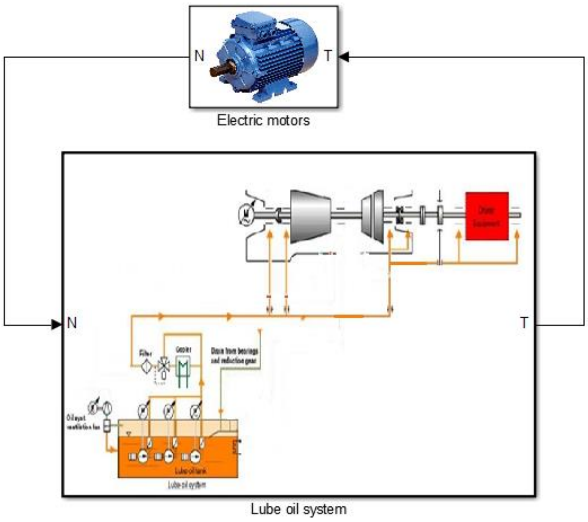


*Figure 14: Final model, integration part*

Based on the described parallel flow and flow feedback principles, the final model is made. This final model has to meet the conditions which are described in section 4.4.4. The final model consist of an integration part and an iterative model. Figure 14 shows the integration model, where the *Lube oil system* block is a subsystem which contains the iterative model. This iterative model is shown in Figure 15 and it can be seen that it contains all the components that were described in chapter 2. In the following paragraphs, the function of each block in the model is explained separately. The centrifugal pumps, electric motors and orifice plate are already explained in the iterative model and integration model and these are the same in the final model.

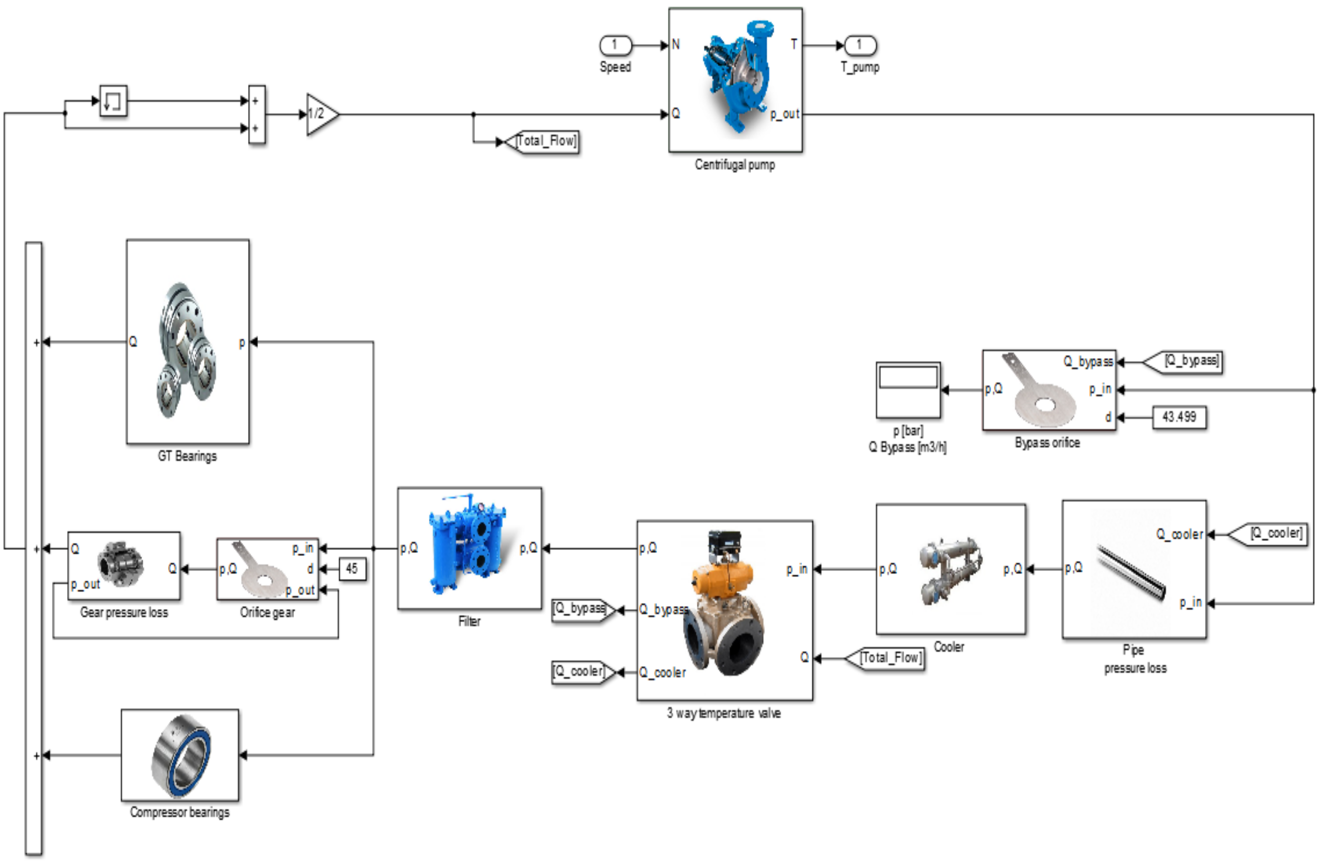


*Figure 15: Final model, iterative part*

 

## 5.1 Pipe pressure loss

The first block behind the centrifugal pumps is the pipe pressure loss block. The distance from the centrifugal pump to the cooler can have a significant length, where the pressure loss in the pipe comes into play. To calculate the pressure loss over this length, a Moody diagram (Figure 16) is used. A Moody diagram relates the Darcy-Weisbach friction factor to the Reynolds number for various values of relative roughness. The Reynolds number for pipe flow is given by [6]:

$$Re = \frac{\rho V D}{\mu}$$

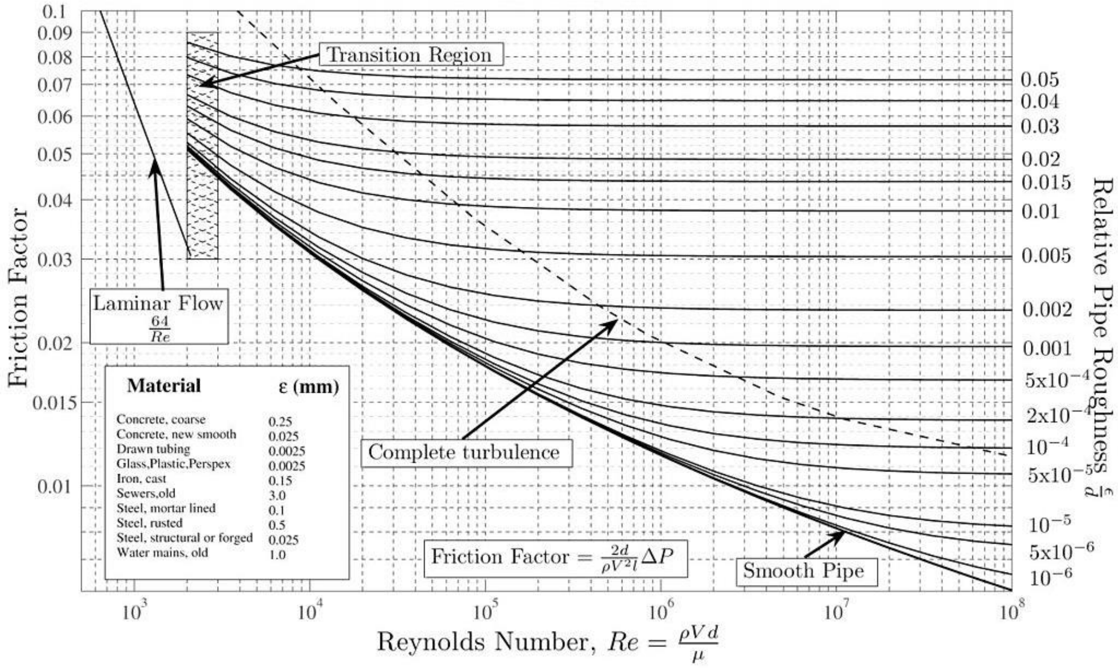


*Figure 16: Moody diagram [7]*

With the friction factor, the pressure loss can be calculated over a pipe of length *L* and diameter *D:*

$$\Delta p = f_D \frac{\rho V^2}{2} \frac{L}{D}$$

The velocity of the fluid is calculated with the incoming flow and the cross-sectional area of the pipe. The only unknown in this equation is the friction factor. Therefore, an equation for the friction factor has to be found. As can be seen in Figure 16, the Moody diagram is split into two flow regimes; laminar flow and turbulent flow. A flow is laminar if the Reynolds number is lower than 2300. For laminar flow, the friction factor is found to be [8, 9]:

$$f_D = \frac{64}{Re}$$

For the turbulent region, where the Reynolds number is larger than 4000, a more complex relation is used. The correlation of Serghides is one of the best explicit approximation of the implicit Colebrook-White equation, which is the best known formula for the friction factor. The correlation of Serghides is [8]:

$$\frac{1}{\sqrt{f_D}} = A - \frac{(B-A)^2}{C - 2B + A}$$

Where

$$A = -2\log_{10}\left[\left(\frac{(\epsilon/D)}{3.7}\right) + \frac{12}{Re}\right]$$
$$B = -2\log_{10}\left[\left(\frac{(\epsilon/D)}{3.7}\right) + \frac{2.51A}{Re}\right]$$
$$C = -2\log_{10}\left[\left(\frac{(\epsilon/D)}{3.7}\right) + \frac{2.51B}{Re}\right]$$

The friction factor can now be calculated for the laminar and turbulent flow. For the transition region, no relations are known. For this model, a linearization is made between the friction factors for laminar and turbulent flow. This done in order to avoid discontinuities in the model. With the described formulas for the friction factor, the Moody diagram can be drawn for each relative roughness. In Figure 17, the Moody diagram is shown for a stainless steel pipe with a roughness of $\epsilon = 0.002\ mm$ [10] and $D = 100\ mm$.

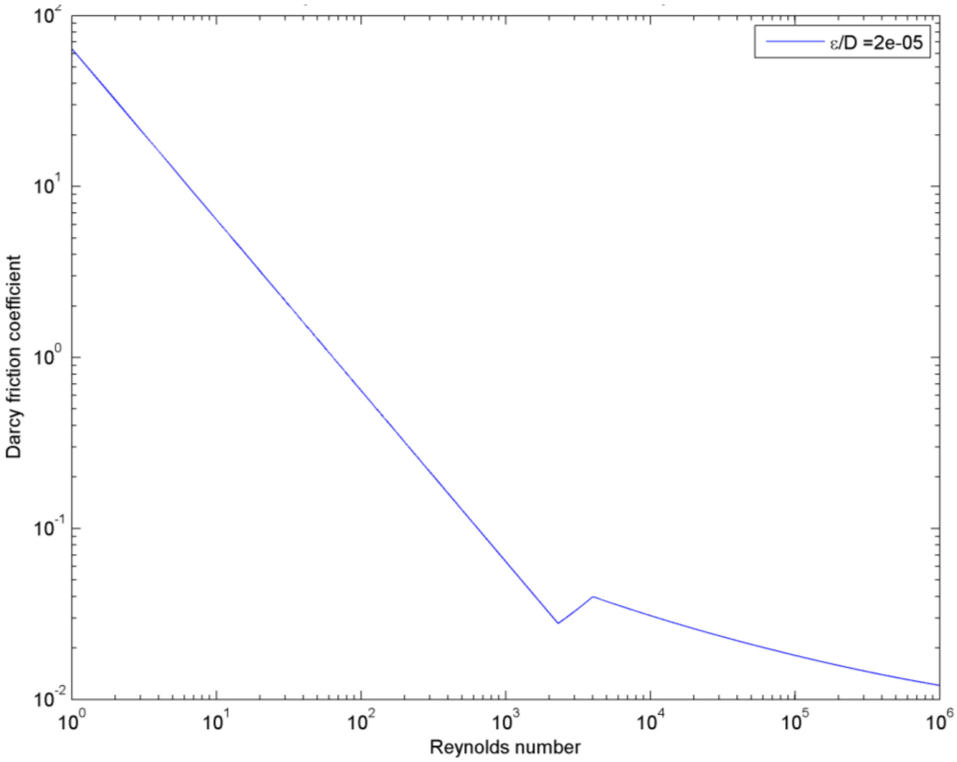


*Figure 17: Approximation Moody diagram*

For each flow, the friction factor can now be determined together with the corresponding pressure loss in the pipe.

## 5.2 Cooler

After the pressure loss in the pipe from the pumps to the cooler is calculated, the flow enters the cooler. As displayed in Table 2, the maximum pressure loss over it is $\Delta p_{max} = 0.869\ bar$ for the design flow. Based on this maximum pressure loss, a quadratic relation is put into the cooler block, since the flow – pressure drop characteristics of most hydraulic elements are approximately quadratic [11] :

$$\Delta p = \Delta p_{max} \left(\frac{Q}{Q_d}\right)^2$$

So, when the flow increases, the pressure loss over the cooler increases quadratic. The design flow for the cooler is equal to the design flow of the centrifugal pumps. The design flow of the centrifugal pump is equal to $Q_d = 96\frac{m^3}{h}$.

## 5.3 3 way temperature valve

The 3 way temperature valve is used to regulate the flow over the cooler and the bypass based on the temperatures of these flows at the valve. Since the temperature of the oil is assumed to be constant in the start-up phase of the system, the valve will divide the flow at a constant rate. This rate is set so that the flow over the cooler is two-third of the total flow and the flow over the bypass one-third of the total flow.

The pressure loss over the valve is calculated with the same relation as for the cooler (section 5.2). The maximum pressure loss for the valve is $\Delta p_{max} = 0.1\ bar$ for the design flow of the centrifugal pumps.

## 5.4 Filter

The total flow in the system then goes through a duplex filter. For the filter it is known that the maximum pressure loss is $\Delta p_{max} = 0.36\ bar$. The filter has the same flow-pressure loss relation as the cooler (section 5.2), but with a different maximum pressure loss.

## 5.5 Gas Turbine bearings

The GT bearings block in the model contains the four bearing of the gas turbine. For the gas turbine bearings it is known that these bearings are pressure fed, which means that the lubricant under pressure is pumped into the bearing. The flow consumption of the bearing depends on the pressure difference over the bearing and is computed using the following equation [12]:

$$Q = \frac{1}{x}\frac{\pi \Delta p r c^3}{3\mu l}(1 + 1.5\epsilon_r^2)$$

Since the geometry of the bearings is not known, some assumptions are made for the radius, clearance and length of the bearings. In the model, also a factor *x* is implemented in the bearings in order to tune the above relation with a constant factor. With this factor, the relation can be fitted to test data if these are known. If the factor *x* is chosen higher than one, the resistance of the bearings is increased and a set pressure difference will result in less flow. For the final model, the factor $x$ is set to one.



 

## 5.6 Compressor bearings

The compressor bearings block in the model contains the two bearings of the compressor. The subsystem under the compressor bearings block is shown in Figure 18. For both the compressor bearings, the flow is directed by an orifice plate in front of the bearings. This flow is again calculated with the pressure difference over the orifices as described in section 4.2.2. To find the pressure between the orifice and the bearing, the pressure loss over the bearing has to be calculated and added to the downstream pressure of the bearing (oil pressure). This represented in Figure 18 with the pressure feedback line from the bearings to the orifice. The pressure loss over the bearings is flow dependent also flow dependent with a quadratic relation.

For one of the bearings it is known that the orifice in front of it is $d = 16.75\ mm$. Furthermore it is known from internal documents that the ratio of the flow between the two compressor bearings is approximately 1:6.8. So the line of compressor bearing 2 gets much less flow than the other line.

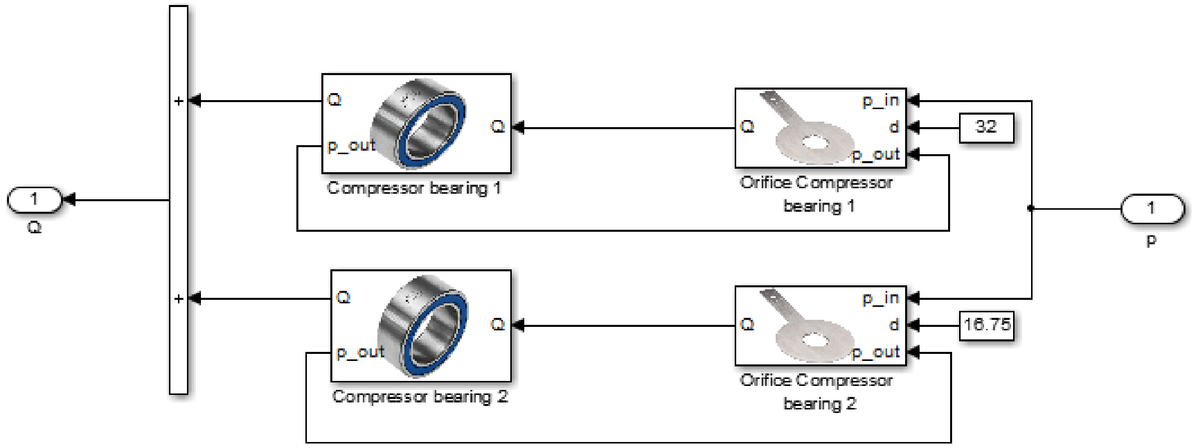


*Figure 18: Subsystem under the compressor bearings block*

## 5.7 Gear

For the gear, it is assumed that the pressure loss is flow dependent with the same quadratic formula as the cooler. The pressure loss over the gear is added to the pressure of the oil in the tank. This is the pressure between the orifice and the gear. The difference between the pressure upstream and downstream of the orifice determines the flow over the gear.

## 5.8 Viscosity

For the pipe pressure loss and the bearings, it can be seen that the viscosity of the oil needs to be known. The viscosity of the oil is strongly dependent on the temperature and in a lesser extent on the pressure. Underneath the subsystems for the bearings and the pipe pressure loss, a *Simulink* block is present which calculates the viscosity for the actual temperature and pressure. From [13], a relation for the dynamic viscosity is found which is dependent on the temperature as well as on the pressure:

$$\mu(p, T) = a \exp\left(\frac{b}{(T + 273.15) - c}\right) \exp\left(\frac{p}{a_1 + a_2 T}\right)$$



 

Where

$$a = 6.33 \cdot 10^5$$
$$b = 879.77$$
$$c = 177.79$$
$$a_1 = 334$$
$$a_2 = 3.256$$

The dynamic viscosity can now be plotted against the temperature and the pressure. The result is shown in Figure 19. This figure shows that the dependency on the temperature has the most effect on the viscosity. For higher temperatures, the dynamic viscosity drops quite fast to an almost constant value.

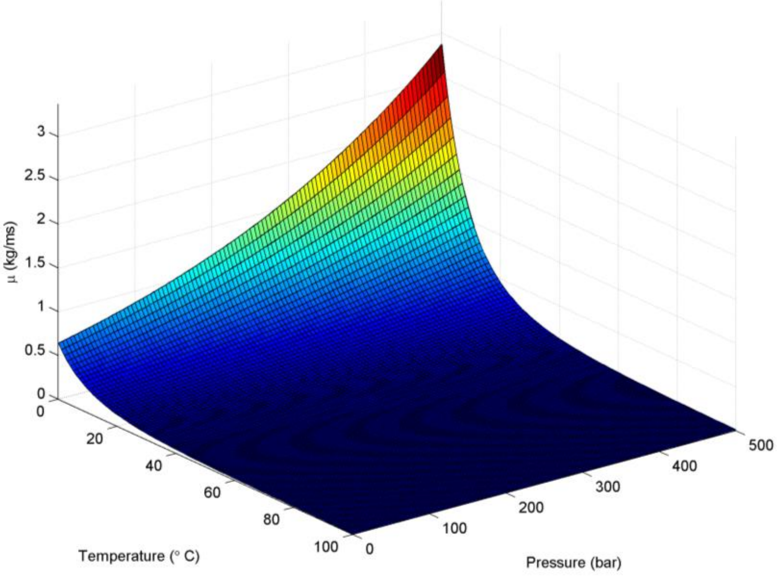


*Figure 19: Dynamic viscosity of ISO VG 46 oil for temperature and pressure*

## 5.9 Static head

The system can also have a static head pressure, which has to be overcome before any flow goes into the system. This can be due to a height difference in the loop, for example when the suction side of the centrifugal pumps is lower than the drain in the lube oil tank. This net static head can be simulated in the centrifugal pumps. This is done by comparing the delivered pressure of the pumps to the net static pressure that has to be overcome. As long as the delivered pressure is lower than the static pressure, the output pressure is set to the inlet pressure (oil pressure). Because this is the same pressure as in the rest of the system, no flow will go through the system, since the flow is based on pressure differences.

As long as the static pressure is not exceeded, the pumps will accelerate and the delivered head pressure for zero flow will increase. As soon as the pumps reach a speed where the delivered head exceeds the static head, the output pressure is the pressure delivered by the pumps minus the static pressure. Summarising, this means that the flow only starts when the static head is overcome.

In this model, the net static head is set to $h_{stat} = 1m$.



 

### 5.10 Bypass orifice

As explained in the system description (chapter 2), there is a bypass line over the cooler with an orifice plate. This orifice plate has to take care of the same pressure drop as the cooler. The diameter of the orifice that corresponds to this pressure drop has to be found.

The pressure upstream the orifice and the pressure downstream the cooler are known after running the model. Also the flow over the orifice and the diameter of the pipe are known, so the only variable in the orifice equation is the bore diameter of the orifice.
When the final model has calculated the flows and pressures in the system , a *MATLAB* script is run which determines the desired bore diameter for the orifice in the bypass. This script reads the data from the model, where the upstream pressure and downstream pressure at steady conditions are used to calculate the flow for all possible diameters for the orifice. These flows are compared to the flow over the orifice and the diameter for which the flow corresponds to the flow in the simulation is the output of this script.
The orifice is also part of the final model. The desired bore diameter can be given as an input and the pressure after the orifice is shown in a display. This can be compared with the pressure after the cooler. The diameter of the orifice can be changed easily and the corresponding pressure after the orifice is calculated.



 

# 6 Results

In Figure 21, the result screen of the model is shown. This model shows the flow and the pressure after each block in the model. It can be seen that the pressure after the filter is equal to $p = 1.8\ barg$. The pressure behind the bearings and the gear are all equal to the oil pressure in the oil tank, which is $p = 0\ barg$.

The centrifugal pumps deliver a pressure of $p \approx\ 4.12\ barg$ at a flow of $Q \approx 154.5 \frac{m^3}{h}$. This flow is larger than the design flow of $Q_d = 96 \frac{m^3}{h}$. So, the operational point of the centrifugal pumps is not at the design point. As described in section 4.4.4, this also to be expected based on the available datasheets for the centrifugal pumps and the other components in the system.

The distribution between the parallel flows is 1:1:2/3 for the gas turbine bearing, the gear and the compressor bearings respectively. This is in accordance with the conditions that were described in section 4.4.4.

## 6.1 Output power

The power that the centrifugal pumps require is calculated with the equations described in section 4.3.2. The required power for operation of the pumps is displayed in a *MATLAB* message box (see Figure 20). For this configuration, the required power is found to be: $P_s = 32.49\ kW$. This is the power that has to be delivered by the electric motors. As can be seen in Attachment 4, the rated output power of the electric motors is $P = 18.5\ kW$ per motor, so $P = 37\ kW$ in total. This is higher than the required power, so the electric motors are capable of delivering the required power.

## 6.2 Bypass orifice diameter

As described in section 5.10, the orifice diameter for the bypass is calculated in order to find the same pressure loss as the pressure loss over the cooler. The diameter for the orifice is also displayed in the *MATLAB* message box, see Figure 20. This diameter is found to be $d = 43.505\ mm$. In Figure 21, it can be seen that the pressure after the cooler and after the orifice is indeed the same for this diameter.

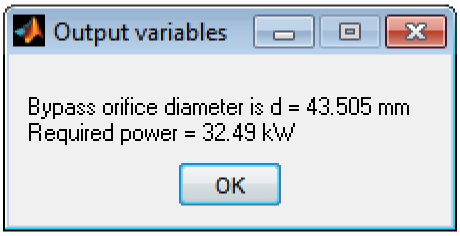


*Figure 20: Message box with results*

 

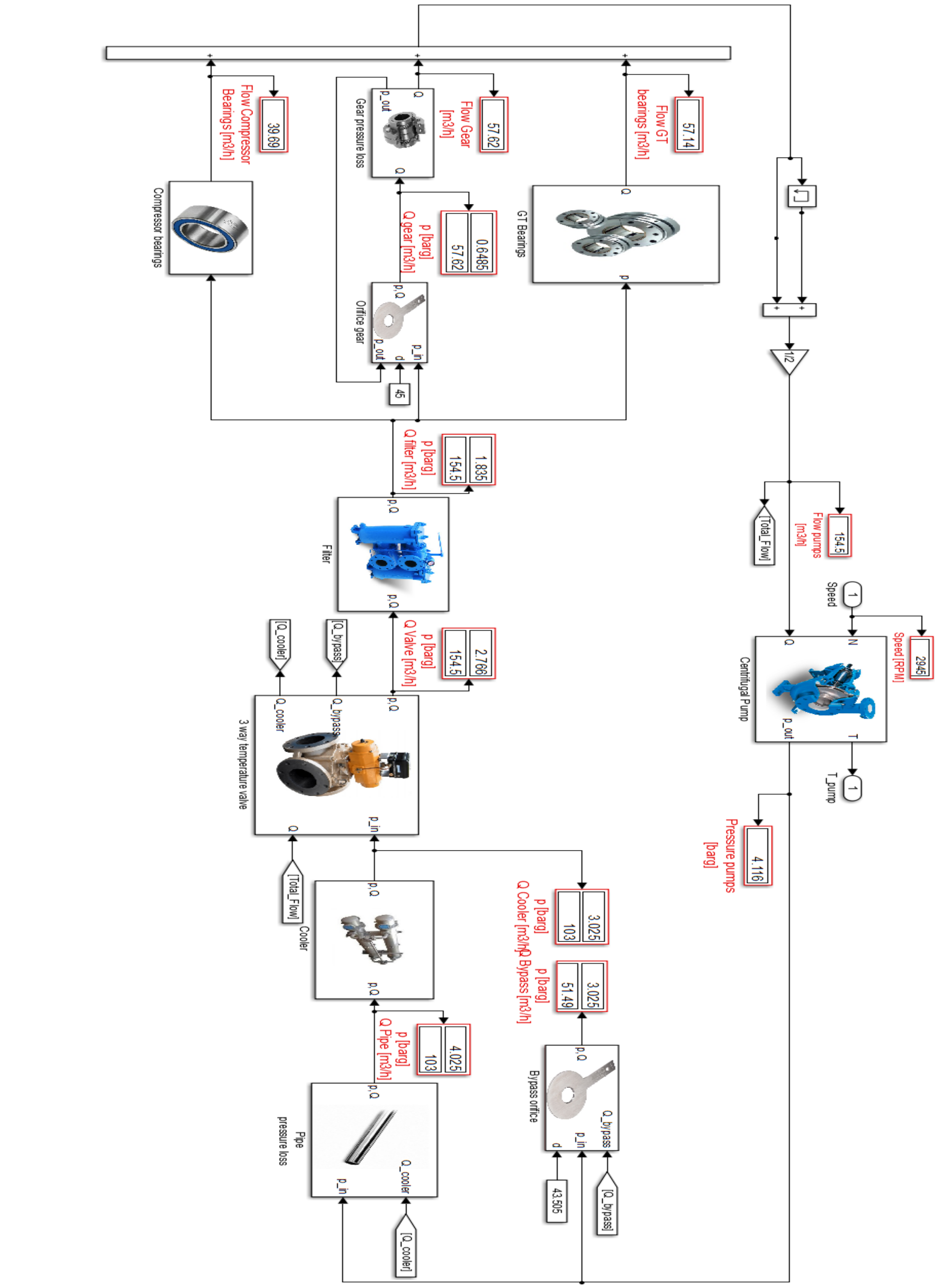


*Figure 21: Result screen*

## 6.3 Torque

When the model reaches the operational speed, the simulation is stopped and some plots are made. In Figure 22, the torque delivered by the electric motor and the torque required by the centrifugal pumps are shown. It can be seen that at the start the required torque by the centrifugal pumps is equal to zero. This is because a static head of $h_{stat} = 1\ m$ is taken into account. As long as this pressure is not delivered by the pumps, there is no flow in the system. From the equations in section 4.3.2 it can be seen that the required torque is then equal to zero.

The total system reaches a constant speed at $t \approx 4.5\ s$. In Figure 22 it is shown that the required torque and the delivered torque intersect each other at that point. So, from there on, the pumps are no longer accelerated.

This relative short time to start the whole system also shows that the assumption made about the constant temperature during start-up is right. In this short amount of time, the bulk temperature of the oil will only change marginally.

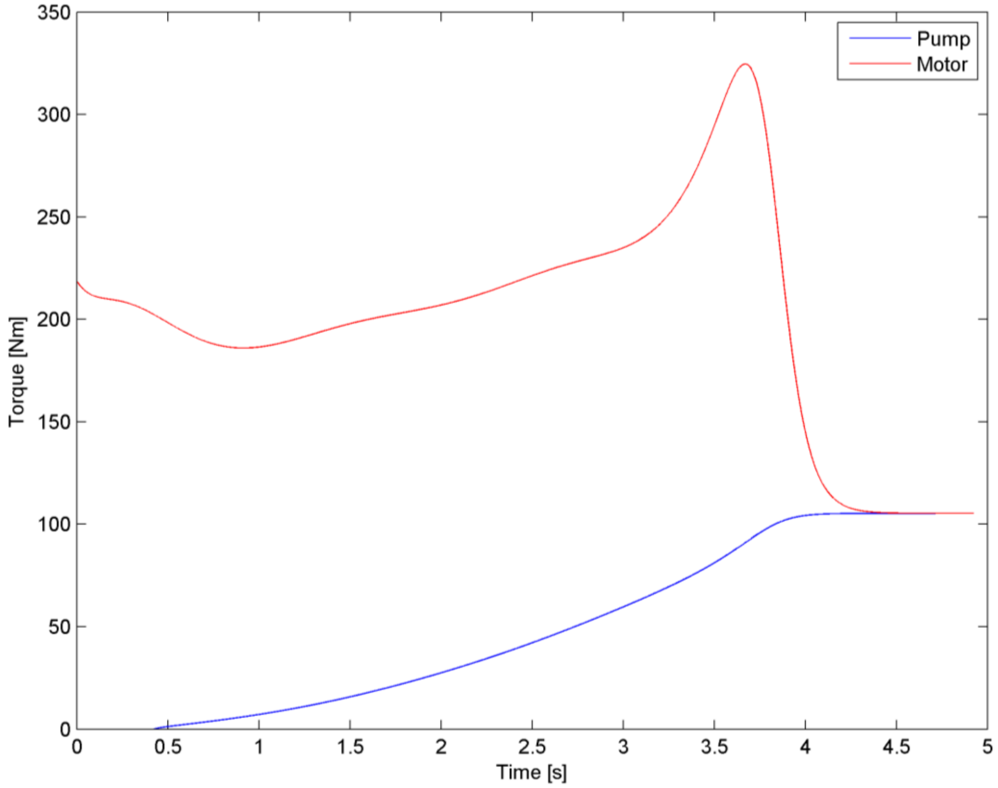


*Figure 22: Torque of the pump and the system*

## 6.4 Flow-head curves

The flow-head curve (Figure 23) is also made when operational speed is reached. This contains the flow-head curve of the centrifugal pumps and the flow-head curve of the system. The curve for the centrifugal pumps is plotted for the operational speed of the pumps, which in this case is $N = 2945\ RPM$. The system curve is plotted in the same figure. This shows that the operational point of the pumps is at $Q \approx 155\ m^3/h$ , where a head pressure of $h \approx 48.7\ m$ is delivered. In this figure, the static head of $h_{stat} = 1\ m$ is also clearly visible. No flow is delivered until this pressure is reached, which can be seen in the line that goes straight to $h = 1\ m$ for zero flow.

The end speed of the pumps is found at $N = 2945\ RPM$, which is also higher than the design speed of $N = 2900\ RPM$ for the pumps. However, when the pumps would be controlled such that the speed is equal to the design speed, the operational point of the pumps would still be at the right side on the curve compared to the design point.

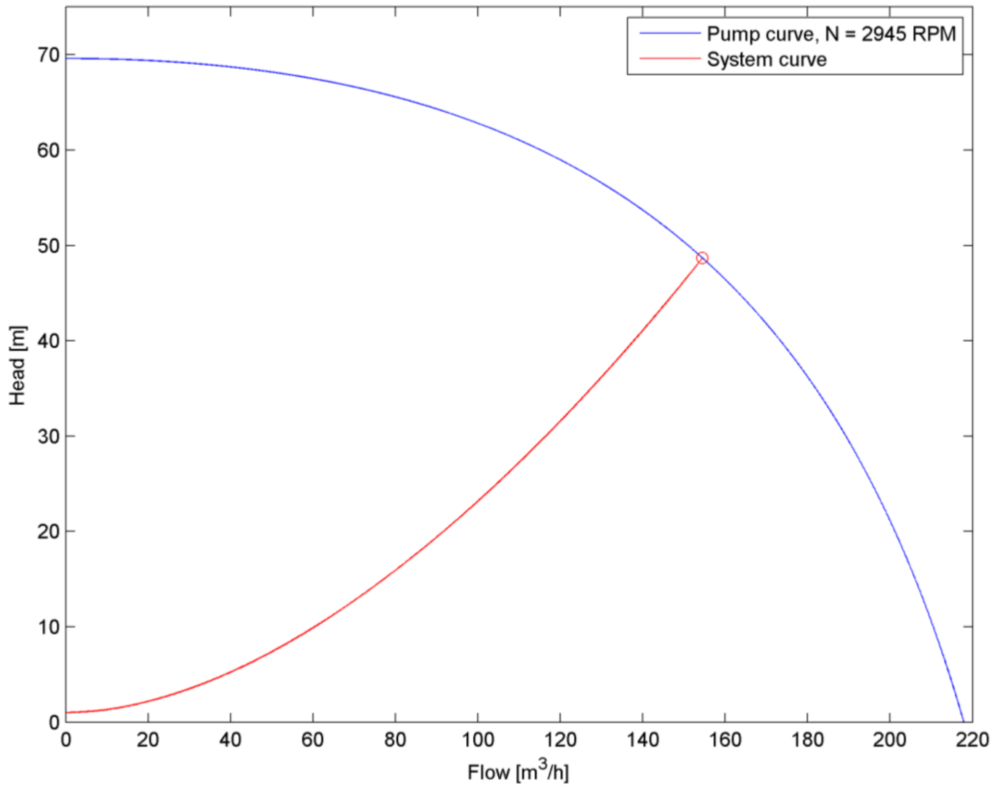


*Figure 23: Flow-head curve of the pump and the system*

## 6.5 Parallel flows

The distribution of the flow over the parallel parts of the system is shown in Figure 24. It can be seen that the distribution over the compressor bearings and the gear has the same kind of curve. This can be explained by the fact that both these flows are regulated by an orifice plate.

In the compressor bearings and the gear the flow increases much faster in the beginning than the gas turbine bearings. But at steady flow, the 1:1:2/3 distribution is clearly visible in this figure. So the gear and the gas turbine bearings get the same amount of flow and the compressor bearings get 2/3 of that flow.

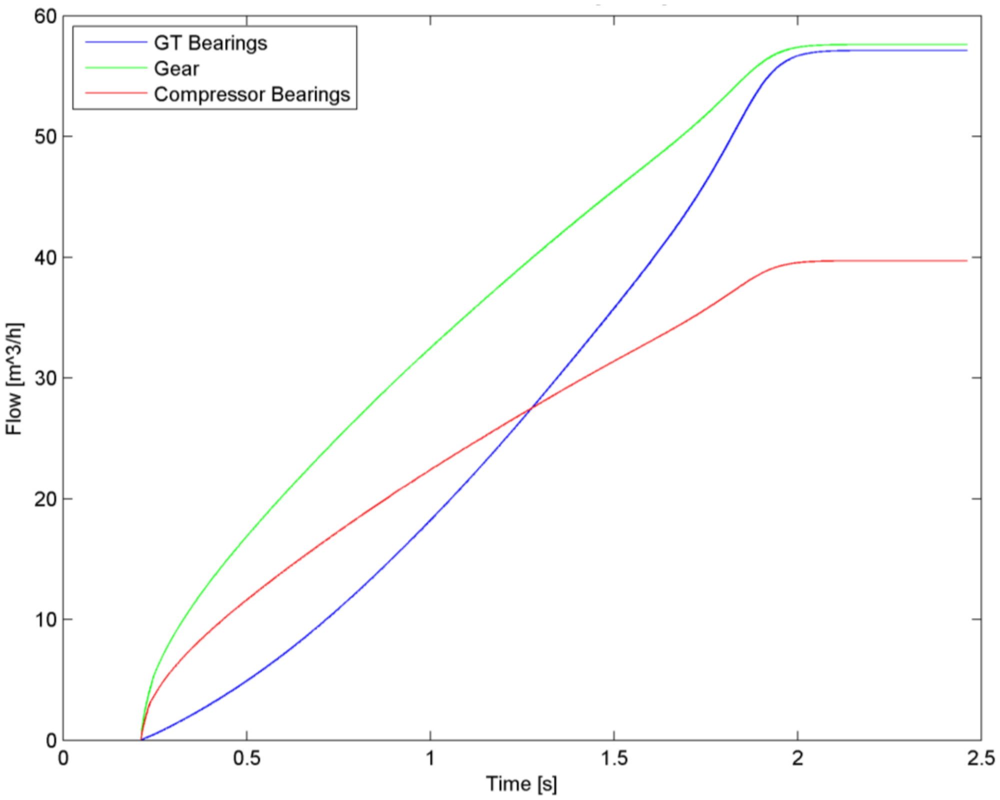


*Figure 24: Flow distribution over bearings and gear*

## 6.6 Compressor bearings

In Figure 25, the flow distribution over the two compressor bearings is shown. It can be seen that the ratio of the flows is found to be approximately 1:6.7.

This result is found for an orifice diameter of $d = 32\ mm$ in front of compressor bearing 1 and the already mentioned orifice diameter $d = 16.75mm$ for compressor bearing 2.

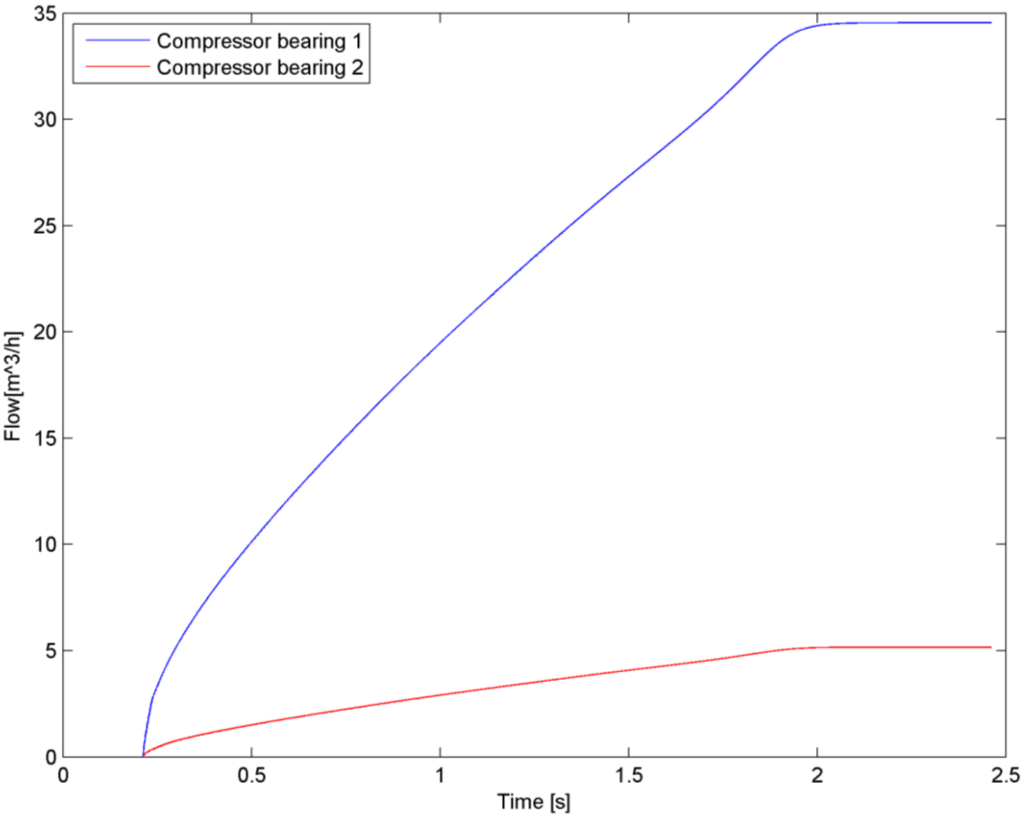


*Figure 25: Flow distribution over the compressor bearings*

 

# 7 Conclusion

As described in the assignment description, the goal of this report is to simulate the physical behaviour of the lube oil system of the SGT-600 with a simplified mathematical model. For several components in the system, some assumptions are made in order to simulate the physical behaviour. Because no test data is available, these assumptions cannot be validated. Therefore, it is not possible to give hard conclusions before these assumptions are validated. It is however possible to give some conclusions based on the available datasheets and the physical behaviour can be compared to what was to be expected.

As described in section 4.4.4, it can be concluded from the available data of the centrifugal pumps and the components in the system, that the system will not operate at the design flow. This also means that the pumps will not operate at their best efficiency point, which is off course undesirable. Even when the pumps would be controlled such that they operate at the design speed, the pumps will not operate at their best efficiency point as was described in section 6.4.

For the pressure after the filter, it is known that the pressure must be $p = 1.8\ barg$. This is also the case in the simulation. For the rest of the system, no test data is known, so it is not possible to compare the pressures in the simulation with test data. This is something that can be done in the future. Furthermore, from datasheets, the distribution between the parallel flows is known for the gas turbine bearings, gear and compressor bearings. In the results (section 6.5) it was shown that the same distribution is found in the simulation.
For the distribution between the two compressor bearings the ratio that was found in datasheets is also found in the simulation. This was shown in section 6.6.
Overall, it can be concluded that the simulation model corresponds with the known data.

It is possible to show the physical behaviour with the final model. This physical behaviour contains the distribution of the flow over parallel components, where the components with the lowest resistance gets the most flow. It also shows the behaviour that the resistance in the system depends on the flow and that the flow depends on the resistance.

Also mentioned in the assignment description is the orifice diameter for the bypass line around the cooler. The goal was to make a simulation model in which a bore diameter for this orifice could be tested. As described in section 5.10, the simulation tool can calculate the desired bore diameter based on the pressure upstream the orifice and the pressure downstream the cooler together with the incoming flow. This diameter can be calculated for every kind of system where a bypass line is used to regulate the pressure drop.



 

## 8 Recommendations

The model represents the physical behaviour of the total system and meets the known conditions, like the pressure after the filter and the distribution of the flows. However, since there is no data available to validate the pressures and flows in the system, not much reasonable conclusions can be drawn from the final model.  So, the first recommendation is to compare the result of the final model to actual test data of the lube oil system. Based on these test data, more reasonable conclusions can be drawn from the final model.

As described in section 4.1, the high pressure part of this lube oil system is not taken into account. For a more complete description of the physical behaviour in the parallel flows after the filter, this high pressure part has to be simulated. For simulating this, a new integration model has to be added to the final model because the high pressure (positive displacement) pumps are also driven by electric motors. The relation between the electric motors for the low pressure part and the electric motors for the high pressure has to investigated before this can be put into the final model. This relation includes the start-up behaviour of both the electric motors. This has to be simulated such that both the low pressure- and high pressure part are at full operation at the same time.

With the described Simulink blocks, a new lube oil system can be modelled easily by connecting the desired blocks. All the blocks themselves can also be modified such that test data can be implemented easily in the blocks.

Further research could be done regarding the role of the temperature in the system. This should be a model where the system operates at a constant speed, and the temperature changes due to operation. The total model should be based on an energy balance, which gives another way of modelling the total system. However, most of the blocks described in this report could be used in order to describe the flows and pressures in the system. The temperature behaviour has to be added in these blocks. The most important components in this model are the cooler and the bearings. This is because the cooler is responsible for the cooling of the oil and the bearings heat up the oil. For the cooler, the amount of heat extracted from the oil has to be simulated.
In this new model, the temperature in the oil tank has to be calculated. This can be done when the flow that enters the oil tank is known together with its temperature. Together with the total oil volume and the bulk temperature, the temperature rise in the system can be calculated. As described in this report, the viscosity of the oil changes significantly with the temperature. By using the described viscosity Simulink block, this viscosity can be found for every temperature.



 

## 9 List of references

[1] I. Karassik, J. Messina, P. Cooper and C. Heald, *Pump Handbook*, Mc Graw Hill, 2007.

[2] International Organization of Standards, “*Measurement of fluid by means of pressure differential devices inserted in circular cross-section conduits running full. Part 1: General principles and requirements,*” 2003.

[3] A. Hughes, *Electric Motors and Drives*, Elsevier, 2006.

[4] P. Girdhar and O. Moniz, *Practical Centrifugal Pumps. Design, Operation and Maintenance*, Elsevier, 2005.

[5] W. Layton, *Introduction to the Numerical Analysis of Incompressible Viscous Flows,* SIAM, 2008.

[6] H. Oertel, *Prandlt-Essential of Fluid Mechanics,* Springer Science & Business Media, 2010.

[7] K. A. Flack and M. P. Schultz, “R*oughness effects on wall-bounded turbulent flows,*” Physics of Fluids, vol. 26, 2014.

[8] M. Asker, O. E. Turgut and M. T. Coban, “*A review of non iterative friction factor correlations for the calculation of pressure drop in pipes*,” 2014.

[9] W. Graebel, *Engineering Fluid Mechanics*, CRC Press, 2001.

[10] F. M. White, *Fluid Mechanics*, Mc Graw Hill, 1998.

[11] V. Tesar, “*Superquadratic behaviour of vortex diodes*,” Pneumatic and hydraulic components and instruments in automatic control, pp. 79-95, 1980.

[12] B. Nisbett, *Mechanical Engineering. Shighley's Mechanical Engineering Design*, Mc Graw Hill, 2006.

[13] D. Knezevic and V. Savic, “*Mathematical modeling of changing of dynamic viscosity, as a function of temperature and pressure, of mineral oils for hydraulics systems,*” 2006.

[14] Sulzer Pumps Ltd, *Centrifugal Pump Handbook*, Elsevier, 2010.



 

# 10 Reference documents

## Attachment 1: Datasheet pumps

*Internal document: 1CS135377_D*

| ALLWEILER | Data sheet<br>NSSV 50-250/01 | Quotation / Offer No. | |
|---|---|---|---|
| | | Project ID | |
| | | Created by | Date<br>2011-09-01 |

**Operating data specification**

| No. | Parameter | | Value | Unit | Parameter | Value | Unit |
|---|---|---|---|---|---|---|---|
| 1 | Fluid | | ISO VG 46 VI95 | | Nominal flow | 96 | m³/h |
| 2 | Solids | Type | | | Nominal head | 61,3 | m |
| 3 | | Weight % | 0 | | Static head | 0 | m |
| 4 | pH-value at t.A | | 0 | | Inlet pressure | 0,0625 | bar |
| 5 | Corrosive components | | | | Altitude | 1000 | m |
| 6 | Operating temperature tw/ts | | 70 / | °C | Available system NPSH | | m |
| 7 | Density at tw/ts | | 0,841 / | kg/dm³ | | | |
| 8 | Vapour pressure at tw/ts | | 0,0003 / | bar | | | |
| 9 | Kin. viscosity at tw/ts | | 13,9 / | mm²/s | | | |

**Pump**

| No. | Parameter | | Value | Unit | Parameter | | Value | Unit |
|---|---|---|---|---|---|---|---|---|
| 10 | Manufacturer | | ALLWEILER | | Impeller type | | Radial impeller | |
| 11 | Pump denomin. | | NSSV 50-250/01 | | Impeller Ø | Max. | 250 | mm |
| 12 | Size | | 50-250/01 | | | designed | 216 | mm |
| 13 | Design | | submerged | | | Min. | 200 | mm |
| 14 | Self-priming | | ☐ Yes | | Flow | Operating point (tw/ts) | 48 | m³/h |
| 15 | Speed | | 2900 | 1/min | | Max.- | 87,1 | m³/h |
| 16 | Max. working pressure | | 5,65 | bar | | Min.- | 0 | m³/h |
| 17 | Max. diff. pressure | | 5,57 | bar | Head | Operating point (tw/ts) | 61,3 | m |
| 18 | No. of stages | | 1 | | | Max.- | 38,8 | m |
| 19 | Circuit/no. of pumps | | Single pumps as parallel circuit 2 | | | Min.- | 67,5 | m |
| 20 | Suction flange | Nominal width | DN 65 | | Head H(Q=0) | | 67,5 | m |
| 21 | | Nominal pressure | 16 | bar | NPSH 3% | | 3,07 | m |
| 22 | | Standard | EN 1092-2 | | Power abs. tw/ts | | 12,2 / | kW |
| 23 | Discharge flange | Nominal width | DN 50 | | Max. shaft power at max. impeller | | | kW |
| 24 | | Nominal pressure | 16 | bar | Efficiency | | 55,5 | % |
| 25 | | Standard | EN 1092-2 | | Calc. power of driver | | 15 | kW |
| | | | | | Make; name | | | |

**Values for the components of NSS/NSSV units**

| No. | Dimensions | | Shaft | | Housing | |
|---|---|---|---|---|---|---|
| 27 | DNA | 100 mm | Type | | Material | |
| 28 | DNA Norm | DIN PN 10/16 | Material | Standard 1.0060 | | |
| 29 | ZET | 630,00 mm | No. intermediate bearings 0 | | | |
| 30 | GET | 600,00 mm | | | | |
| 31 | ZD | 480,00 mm | | | | |
| 32 | LR | 170,00 mm | | | | |
| 33 | Hgeo | 0,65 m | | | | |
| 34 | **Component** | | **Length about** | **Friction loss head** | **Velocity** | |
| 35 | Strainer gasket | | 70 mm | 1,152 m | cs | 5,04 m/s |
| 36 | 90°Elbow | | 76 mm | 3,447 m | cd | 13,58 m/s |
| 37 | Diffuser | | 100 mm | 4,448 m | ca | 3,40 m/s |
| 38 | Check valve | | 22 mm | 3,291 m | | |
| 39 | Pipe | | 603 mm | 0,085 m | | |
| 40 | Elbow / delivery | 0 ° | 0 mm | 0,000 m | | |
| 41 | | | | | | |
| 42 | | | | | | |

Remarks:

V2.0.6



 

Power data referred to: ISO VG 46 VI95

| | Q | H | P | V/e | Temp | Density | rated Torque | Speed |
|---|---|---|---|---|---|---|---|---|
| 1) | 48,00 m³/h | 61,28 m | 12,17 kW | 13,8 mm²/s | 70,0 °C | 0,84 kg/dm³ | 40,1 Nm | 2900 1/min |
| 2) | | | | | | | | |

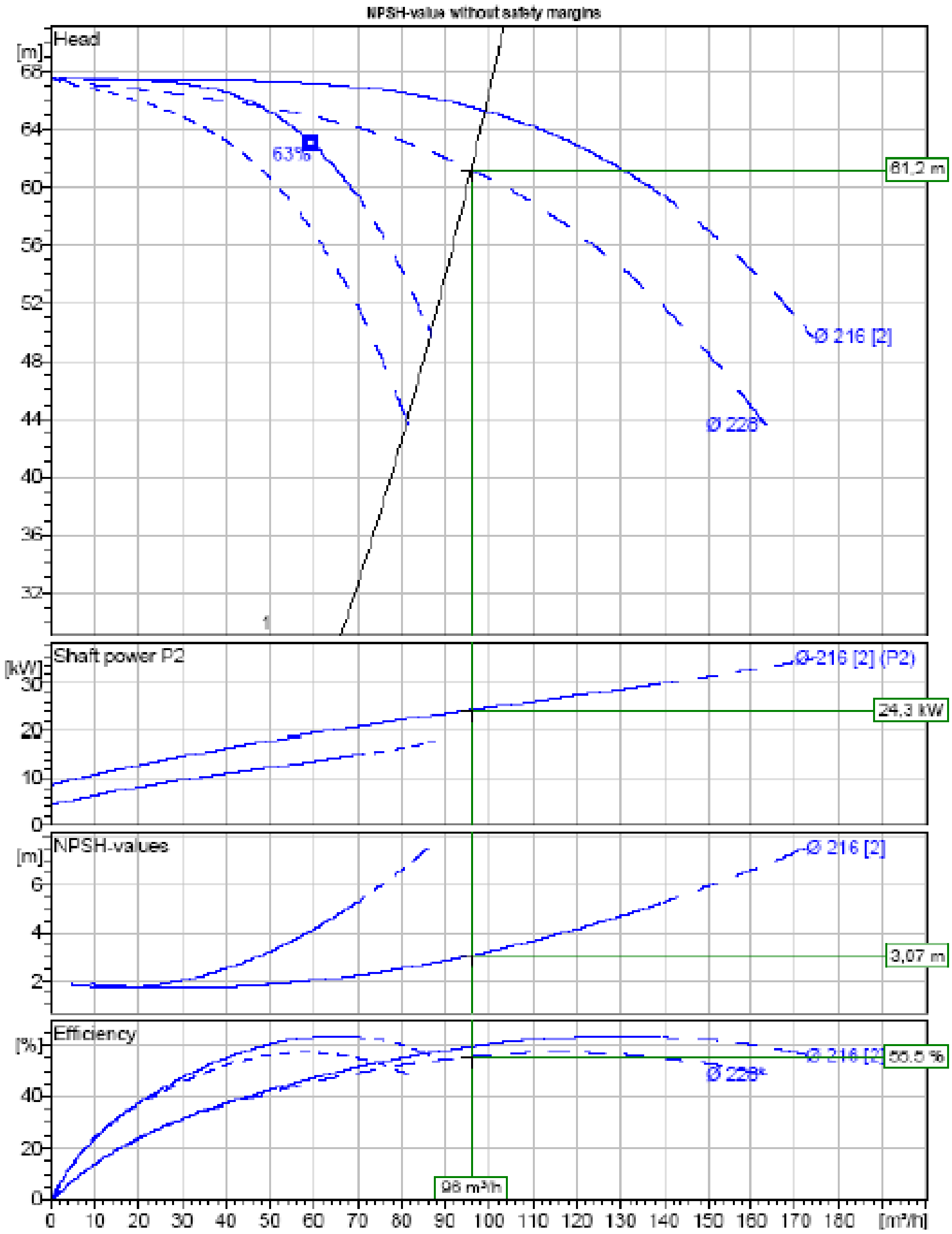




 

## Attachment 2: Centrifugal pumps approximation

In order to approximate the flow-head curve of the centrifugal pump, an approximation method is used which needs the design and maximum conditions (head and flow) and the stable flow range of the centrifugal pump as input. The method used has been developed by G. de Boer, project coordinator of this report.

With the shut-off head and the operational head, the percentage head rise from the design point to the maximum head is calculated.

$$h_{\%} = \frac{h_{so} - h_d}{h_d} \cdot 100\%$$

The stable flow range states at which percentage of the operational flow, the derivative is equal to zero. For this centrifugal pump this is at zero flow, so:

$$s = 0$$

Furthermore, the ratio between the maximum flow and the design flow is used for the approximation.

$$r = \frac{Q_{max}}{Q_{op}}$$

With this input, the equation for the head pressure as a function of the flow is:

$$h = C_3 Q + C_2 \ln(1 - C_1 Q) + C_4$$

Where the coefficients of this equation are:

$$C_1 = \frac{1}{r Q_d}$$

$$C_2 = \frac{\frac{h_{\%}}{100} h_d}{\ln(1 - C_1 s Q_d) - \ln(1 - C_1 Q_d) - \frac{(1-s)C_1}{\left(1 - s Q_{op} C_1\right) Q_d}}$$

$$C_3 = \frac{C_2 C_1}{1 - s Q_d C_1}$$

$$C_4 = h_{op} - C_3 Q_d - C_2 \ln(1 - C_1 Q_d)$$

Note: in the equations above, the flow is given in $\left[\frac{m^3}{h}\right]$ instead of $\left[\frac{m^3}{s}\right]$. This is done in order to match the units of the datasheet.

The result of approximating the flow-head curve this way is that the curve always intersect with the design point and that the derivative at zero flow is equal to zero. In Figure 26, the result of the approximation is shown together with data points from the datasheet.

A big advantage of approximating the flow-head curve in this way is that it is applicable for other centrifugal pumps as well if the input as described above is known for the pump.

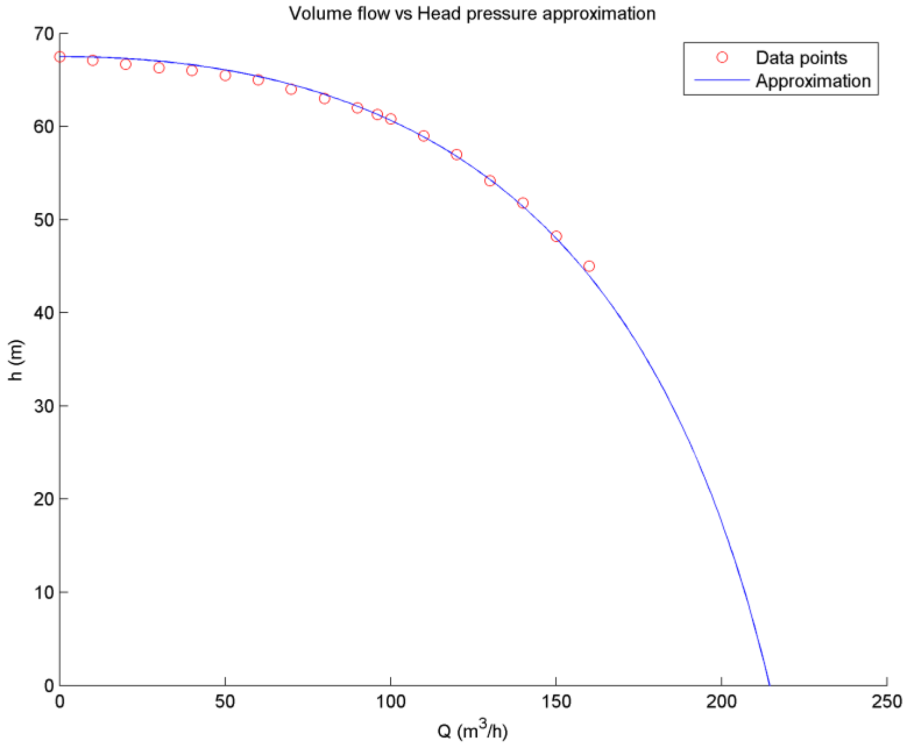


*Figure 26: Approximation flow-head curve of the pumps*

## Attachment 3: Orifice plate

As described in section 4.2.2, the orifice equation is given by:

$$Q = CA_{orif}\sqrt{\frac{2(p_1 - p_2)}{\rho}}$$

In this equation, $C$ is known as the flow coefficient. This flow coefficient is formed by the discharge coefficient ($C_d$) and the *velocity of approach factor*, which is in the numerator of the equation [2]:

$$C = \frac{C_d}{\sqrt{1-\left(\frac{d}{D}\right)^4}} = \frac{C_d}{\sqrt{1-\beta^4}}$$

The discharge coefficient is given with the following, large equation [2]:

$$C_d = 0.5961 + 0.0261\beta^2 - 0.216\beta^8 + 0.000521\left(\beta\cdot\frac{10^6}{Re}\right)^{0.7}$$
$$+ (0.0188 + 0.0063A)\beta^{3.5}\cdot\left(\frac{10^6}{Re}\right)^{0.3}$$
$$+ (0.042 + 0.08\epsilon^{-10L_1} - 0.123\epsilon^{-7L_1})\cdot(1-0.11A)\cdot\left(\frac{\beta^4}{1-\beta}\right)$$
$$- 0.031(M_2 - 0.8M_2^{1.1})\beta^{1.3}$$

Where

$$\beta = \frac{d}{D}$$
$$Re = \frac{\rho V D}{\mu}$$
$$\epsilon = 1 \quad \text{for incompressible fluids}$$
$$A = \left(\frac{19000\beta}{Re}\right)^{0.8}$$
$$M_2 = \frac{2L_2}{1-\beta}$$
$$L_2 = \begin{cases} 0 & \text{For corner tappings} \\ 0.47 & \text{For D and D/2 tappings} \\ \frac{0.0254}{D} & \text{For flange tappings} \end{cases}$$
$$L_1 = \begin{cases} 0 & \text{For corner tappings} \\ 1 & \text{For and D/2 tappings} \\ \frac{0.0254}{D} & \text{For flange tappings} \end{cases}$$

For sake of simplicity, an approximation is made for this large equation, where only the first two terms of the large equation are taken into account:

$$C_d = 0.5961 + 0.0261\beta^2$$

This coefficient gives a constant value for the discharge coefficient, based on the diameters of the pipe and the orifice. The difference between the approximation and the total equation for the discharge coefficient is plotted in Figure 27 ,for the situation where $d = 50mm$ and $D = 100\ mm$ and $L1 = L2 = 0.0254/D$. The absolute difference is found to be in the order of $\sigma(10^{-3})$. This shows that the approximation used is accurate enough for the purpose of this report.

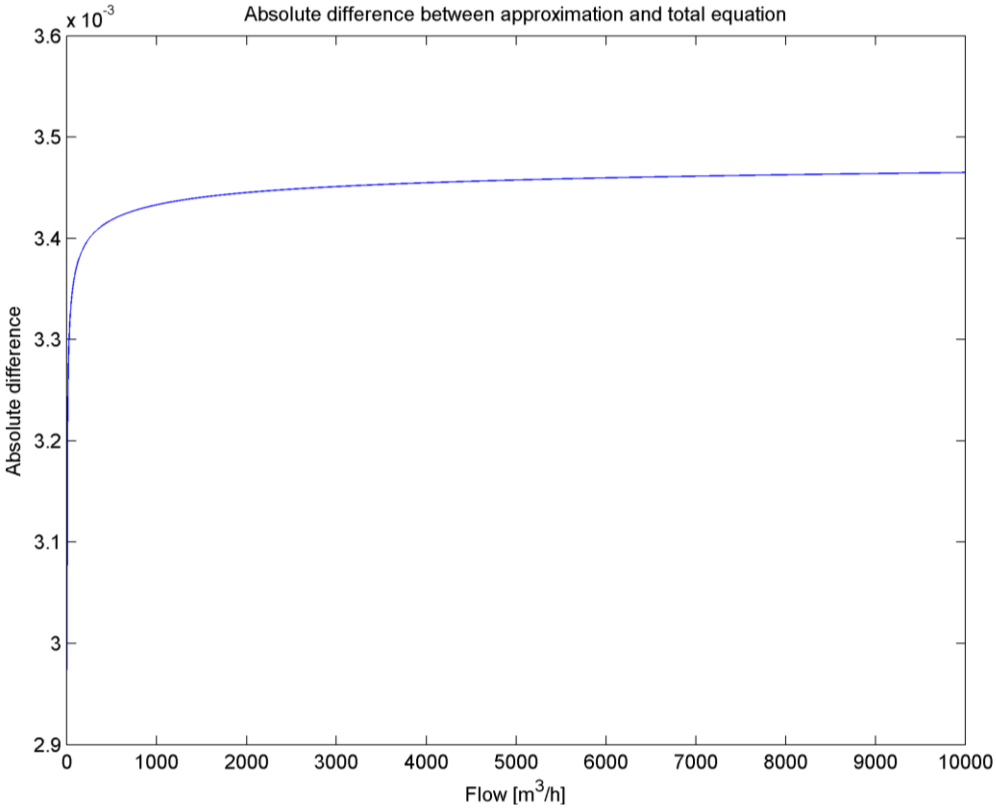


*Figure 27: Difference of the discharge coefficient for approximation and total equation*

The total orifice equation then becomes:

$$Q = \frac{C_d}{\sqrt{1-\beta^4}} A_{orif} \sqrt{\frac{2(p_1 - p_2)}{\rho}}$$

With the approximation for the discharge coefficient:

$$Q = \frac{0.5961 + 0.0261\beta^2}{\sqrt{1-\beta^4}} A_{orif} \sqrt{\frac{2(p_1 - p_2)}{\rho}}$$

If it is desired to calculate the pressure drop over an orifice plate, the equation can be rewritten as:

$$\Delta p = \left(\frac{Q}{C \cdot A_{orif}}\right)^2 \cdot \left(\frac{\rho}{2}\right)$$

 

## Attachment 4: Datasheet electric motor

*Internal document: E1A1455180_B_Zcina*

SIEMENS

**Datenblatt**
data sheet

| | | | |
|---|---|---|---|
| Motor Typ / Motor type | DNGK-200LR-02M | MLFB | 1PS4206-1BD94-3AA0-Z |
| IEC-Baugröße / IEC-Size: 200L; Polzahl / Number of poles: 2 | | Meßflächen-Schalldruckpegel LpA in db(A) nach DIN 45635 / Average sound pressure level LpA acc. DIN 45 635 | Leerlauf / No load: 75+3; Last / Load: |
| Bauform / Mounting design: IM V1; Schutzart / Type of enclosure: IP 55 | | | |
| Kühlart / Cooling type | IC 411 | Drehrichtung (von AS gesehen) / Direction of rotation (viewed from DE) | beide / both |
| Ex-Schutzart / Ex-Protective system | II 2 G Ex de IIB T3 Gb | Lager AS/BS / Bearing DE/NDE | 6312 /C3 / 6312 /C3 |
| Betriebsart / Duty type: S1-7/9; Einschaltung / Starting: direkt / d.o.l | | Schmiermittel / Lubricant | Shell Gadus S3 T100 2 |
| Umgebungstemperatur / Ambient temperature KT | -20/+70 °C | Schmierart / Type of lubrication | Nachschmierung / Regreasing |
| Wärmeklasse / Thermal classification: 155(F); Ausnutzung / Utilisation: 130(B) | | Nachschmierfrist / Relubrication term: 2800 h | Menge / Quantity: 20 g |
| Therm. Wicklungsschutz / Therm. winding protection | 3KL130 / 3PTC130 | Massblatt Nr.: / Outline dimension drawing No. | MLD20-0224-L |
| Therm. Lagerschutz / Therm. bearing protection | --- | Lage des Klemmenkastens / Location of terminal box | seitlich / lateral |
| Bemessungsleistung / Rated output | 18,5 kW | Klemmenzahl / Number of terminals | 6+2 |
| Bemessungsspannung / Rated voltage | 270 V | Kabeleinführungsgew. / Cable entry thread | 2xM50x1,5+1xM20x1,5 |
| Schaltung / Connection | D | Gewicht ca / Net weight approx. | 335 kg |
| Frequenz / Frequency: 50 Hz c/s; Drehzahl / Speed: 2971 1/min rpm | | Sonstige Daten und Bemerkungen: / Additional data and remarks: | |
| Bemessungsstrom / Rated current (CR) | 48 A | am Umrichter / at inverter: M=quad. P=17kW ( ~42,5A ) 1:10 KL für Alleinschutz / PTC for sole protection | |
| Anlaufstrom / Starting current | 690 % | | |
| Leistungsfaktor (cos φ) / Power factor | 4/4: 0,90; 3/4: 0,89; 1/2: 0,86 | | |
| Wirkungsgrad (%) / Efficiency nach/ acc. to EN60034-2-1 | 4/4: 91,7; 3/4: 91,7; 1/2: 90,5 | | |
| Bemessungsmoment / Rated torque ($M_N$) | 59 Nm | | |
| Anzugsmoment / Starting torque $M_A / M_N$ = | 185 % | MBV21AP005-M01 MBV22AP005-M01 MBV23AP005-M01 | |
| Kippmoment / Break-down torque $M_K / M_N$ = | 275 % | | |
| Läuferklasse / Rotor class | HS5 | | |
| Trägheitsmoment / Moment of inertia | 0,2 kgm² | Motor-Nr./Motor-No. 3438375-377 BVS 13 ATEX E 012X | |
| Drehmomentkurve-Nr. / Torque characteristic-No. | --- | AB/EP-Nr. | 8923557-010 / L1-100048976 |

| | Tag; Date | Name; Name | Toleranzen nach/ Tolerances acc. to DIN EN 60 034-1 | Nr. / No. DBL 71746 |
|---|---|---|---|---|
| Bearb.; Design. | 21.08.14 | Z0024UZP-KIPA | | |
| Gepr.; Checked | 21.08.14 | Z001MKXU-HATH | | |



 

SIEMENS

## Strom-Drehmoment-Kennlinie

### Current-Torque-Curve

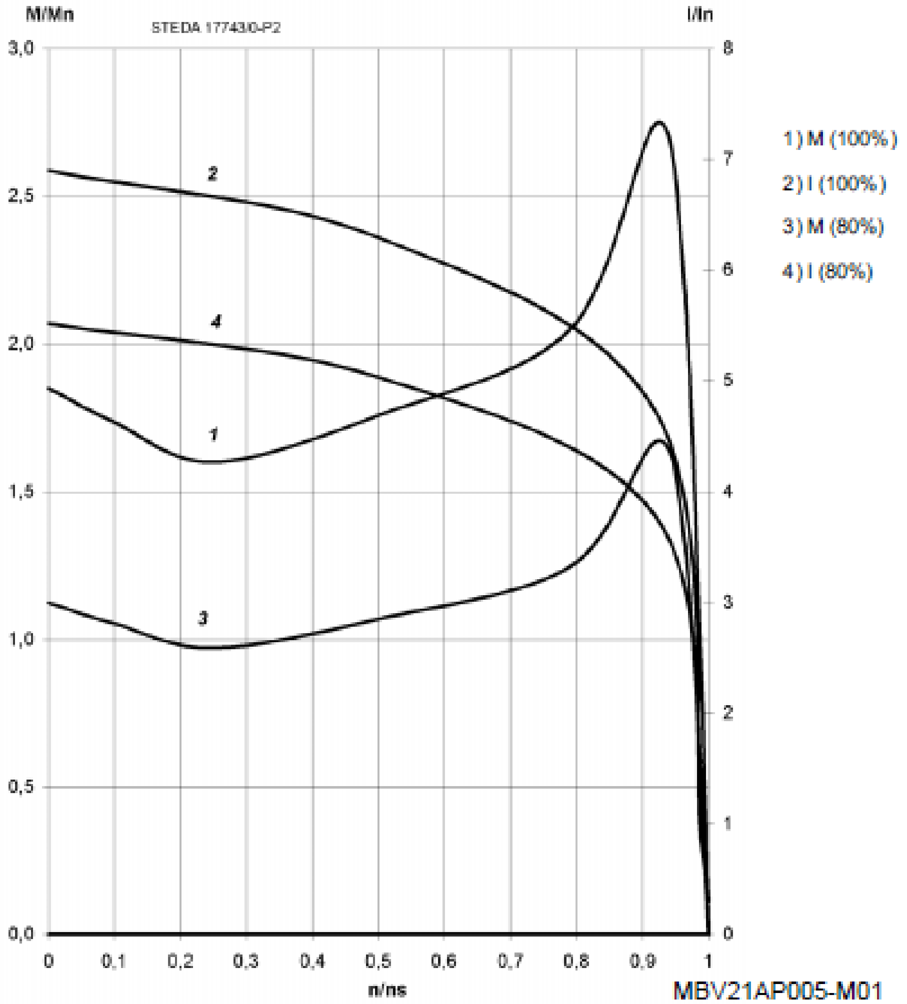


MBV21AP005-M01
MBV22AP005-M01
MBV23AP005-M01

M/Mn = Starting torque/Rated torque
I/In = Starting current/Rated current
n/ns = Full load speed/Synchronous speed

Bemerkung
Remark

| | | | | | |
|---|---|---|---|---|---|
| Bemessungsspannung / Rated voltage | 270 V - D | Bemessungsleistung / Rated output | 18,5 kW | MLFB | 1PS4206-1BD94-3AA0-Z |
| Drehzahl / Speed | 2971 1/min rpm | Bemessungsstrom / Rated current (CR) | 48 A | Motor Typ / Motor type | DNGK-200LR-02M |
| Frequenz / Frequency | 50 Hz c/s | Leistungsfaktor / Power factor | 0,90 | Motor-Nr. / Motor-No. | 3438375-377 |
| Polzahl / Number of poles | 2 | Bemessungsmoment / Rated torque | 59 Nm | | |

| | Tag; Date | Name; Name | Toleranzen nach/Tolerances acc. to | Nr. / No. |
|---|---|---|---|---|
| Bearb.; Designed | 21.08.14 | Z0024UZP-KIPA | DIN EN 60 034-1 | SDK 26004 |
| Gepr.; Checked | 21.08.14 | Z001MKXUHATH | | |

 

## Attachment 5: Datasheet compressor bearings

*Internal document: OilflowCalculatoin5684880674665712417*

In this sheet it can be seen that the pressure upstream the compressor bearings is equal to $p = 1.8\ barg$. This pressure is equal to the pressure downstream the filter.

Result Data "Compressor STC-SV1 (in Train: Train 1)"

| Input Data and Resulting Boundary Conditions | | | |
|---|---|---|---|
| **Oil** | | | |
| Quality / Viscosity | ISO VG | - | ISO VG 46 |
| Inlet Temperature | $T_E$ | °C | 45 |
| Permissible Temperture Rise | $\Delta_T$ | °C | 25.00 |
| Supply Pressure (Header) | $p_H$ | barg | 1.80 |
| **General** | | | |
| Design Speed | $n_{100\%}$ | rpm | 3643 |
| Max. Continous Speed | $n_{105\%}$ | rpm | 3825 |
| Driver Type | | - | gasTurbine |
| Heating for Casing Cover | | - | no |